Comparative spring mechanics in mantis shrimp

S. N. Patek*, M. V. Rosario* and J. R. A. Taylor+

*Department of Biology, Organismic and Evolutionary Graduate Program, University of Massachusetts Amherst, MA 01003 U.S.A.

+Department of Biology, Indiana University-Purdue University, Fort Wayne, IN 46805-1499 U.S.A.

Corresponding author:

S. N. Patek

Department of Biology

University of Massachusetts

Amherst, MA 01003 U.S.A.

Telephone: (413) 577-4426

Fax: (413) 545-3243

Email: patek@bio.umass.edu

ABSTRACT

Elastic mechanisms are fundamental to fast and efficient movements. Mantis shrimp power their fast raptorial appendages using a conserved network of exoskeletal springs, linkages and latches. Their appendages are fantastically diverse - ranging from spears to hammers. We measured the spring mechanics of 12 mantis shrimp species from 5 different families exhibiting hammer-shaped, spear-shaped and undifferentiated appendages. Across species, spring force and work increase with size of the appendage and spring stiffness is not correlated with size. Species that hammer their prey exhibit significantly greater spring resilience compared to species that impale evasive prey (i.e., "spearers"); mixed statistical results show that species that hammer prey also produce greater work relative to size during spring loading compared to spearers. Disabling part of the spring mechanism, the "saddle", significantly decreases spring force and work in three smasher species; cross-species analyses show a greater effect of cutting the saddle on the spring force and stiffness in species without hammers compared to species with hammers. Overall, the study shows a more potent spring mechanism in the faster and more powerful hammering species compared to spearing species while also highlighting the challenges of reconciling within-species and cross-species mechanical analyses when different processes may be acting at these two different levels of analysis. The observed mechanical variation in spring mechanics provides insights into the evolutionary history, morphological components and mechanical behavior that were not discernible in prior single-species studies. The results also suggest that, even with a conserved spring mechanism, spring behavior, potency and component structures can be varied within a clade with implications for the behavioral functions of power-amplified devices.

Key words: Stomatopoda, spring, force, biomechanics, predation

INTRODUCTION

Elastic mechanisms are the biomechanical foundation for rapid and efficient organismal movements. The extraordinary efficiency of kangaroo hopping (Alexander, 1988; Alexander and Vernon, 1975), the extreme accelerations of cellular jellyfish stingers (Nüchter et al., 2006), and the tremendous speeds of termite jaws, trap-jaw ant mandibles and snapping shrimp appendages (Lohse et al., 2001; Patek et al., 2006; Seid et al., 2009; Spagna et al., 2008; Versluis et al., 2000) are all driven by the storage and rapid release of elastic potential energy. The field of elastic biomechanics is rich with analyses of the energetics, mechanics and material behavior of these spring-based systems (Alexander, 1988; Alexander, 2003; Patek et al., 2011; Roberts and Azizi, 2011; Vogel, 2005; Wainwright et al., 1976), yet there is far less understanding of how these systems have been modified over evolutionary history to achieve the remarkably diverse functions that are in evidence today. The goal of this study is to test how mechanical spring parameters co-vary across species, specifically through a phylogeny-based comparative analysis of the elastic feeding mechanism in mantis shrimp (Crustacea: Stomatopoda).

Comparative studies of elastic systems show substantial variation in elastic mechanisms and behavior. Comparisons of wallabies and kangaroos reveal that elastic properties such as safety factors and energy storage may correlate with habitat features (McGowan et al., 2008b); for example, wallabies that hop rapidly in open habitats store substantially more elastic strain energy in their tendons than do wallabies that maneuver over steep, rocky cliffs (McGowan et al., 2008a). A comparison of pigeon and owl feathers reveals that the flexibility of feather shafts is more greatly impacted by the second moment of area than by changes in Young’s modulus (Bachmann et al., 2012). Two elastic seed dispersers - bittercress (Brassicacea, *Cardamine parviflora*) and jewelweed (Balsaminaceae, *Impatiens capensis*) - use elastic energy stored in the seed pods' valves to explosively collapse while releasing the seeds (Hayashi et al., 2009). Their elastic energy transfer and efficiency was compared and the distance disperser (*C. parviflora*) has greater dispersal distance and efficiency than *I. capensis* although the actual spatial pattern of dispersal is not significantly different between these two species (Hayashi et al., 2009; Hayashi et al., 2010). A comparative study of six arachnid species shows that elastic behavior of arachnid legs is achieved through morphological changes, specifically by shifting the configurations of elastic transarticular sclerites and internal pressure (Sensenig and Schultz, 2004; Sensenig and Shultz, 2003). Thus, organisms vary elastic mechanics in a variety of ways, yet studies are still needed that incorporate a broad sample of closely related species in the context of phylogenetic relationships in order to rigorously test the associations between biomechanical features and functional variation.

Mantis shrimp use an elastic mechanism to power a diversity of appendage shapes, ranging from spiny spears to bulbous hammers (Ahyong, 2001; Ahyong and Harling, 2000; Caldwell, 1975; Caldwell and Dingle, 1976) (Figs. 1&2). The morphology of the appendage tends to correspond to its function: elongate, spear-shaped appendages ("spearers") are typically used for sit-and-wait predation of evasive prey (deVries et al., In press), whereas a bulbous hammer at the base of the dactyl ("smashers") is associated with smashing of hard-shelled prey (Weaver et al., 2012). A third category, consisting of the basal *Hemisquilla* spp., has undifferentiated appendages (a sharp dactyl tip and non-bulbous dactyl-heel) which are used for dislodging hard-shelled prey (e.g., limpets). Smasher strikes occur within milliseconds, can reach speeds of over 20 m s^{-1} (Burrows, 1969; Burrows and Hoyle, 1972; Patek et al., 2004) and can strike with impact forces of over 1000 N (thousands of times their body weight) coupled with the considerable forces caused by cavitation bubble collapse (Patek and Caldwell, 2005).

Spearer strikes are much slower (1-7 m s^{-1}) and do not generate cavitation (deVries et al., In press). *Hemisquilla* spp. have strike durations of approximately 4.5 ms and generate cavitation (unpubl. data).

The strike mechanism operates with a combination of large, slowly contracting muscles, latches, linkages and exoskeletal elastic structures (Claverie et al., 2011; Patek et al., 2004; Patek et al., 2007; Zack et al., 2009). In preparation for a power-amplified strike, the lateral extensor muscle slowly contracts while flexor muscles engage a pair of latches to prevent movement (Burrows, 1969; Burrows and Hoyle, 1972; McNeill et al., 1972). During this contraction, elastic energy is stored in the compression of a stiff, exoskeletal structure distal-laterally positioned on the merus segment (the “meral-V”) and a saddle-shaped structure on the dorsal surface of the merus (the “saddle”) (Fig. 1) (Patek et al., 2004; Patek et al., 2007; Zack et al., 2009). When the animal is ready to strike, the flexor muscles relax, release the latches, and the stored elastic energy is delivered via a linkage mechanism that couples the meral-V and saddle extension (energy release) to the propulsion of the dactyl and propodus rapidly toward the target (Burrows, 1969; Burrows and Hoyle, 1972; McNeill et al., 1972; Patek et al., 2004; Patek et al., 2007; Zack et al., 2009).

The evolutionary history of spring mechanics in mantis shrimp has been unstudied until now, with prior studies focusing on single species mechanics in the smashers, *Gonodactylaceus falcatus*, *Gonodactylus smithii* and *Odontodactylus scyllarus* (Claverie et al., 2011; McHenry et al., 2012; Patek et al., 2004; Patek et al., 2007; Zack et al., 2009). Recent stomatopod phylogenies show that the undifferentiated *Hemisquilla* spp. sit at the root of the tree with spearers emerging from these taxa and smashers occurring as a single origin within the spearers (Ahyong and Jarman, 2009; Porter et al., 2010). The components of the elastic system are visible as early as the Paleozoic (*Tyrannophontes gigantion*) with a saddle discernable in fossils (Schram, 2007).

The mantis shrimp's use of a catapult-type mechanism sets the stage for several predictions about the evolutionary variation of elastic mechanisms that should also be applicable to other elastic systems. First, fundamental spring properties, such as spring force, spring stiffness and spring work, should scale positively with body size or the size of the elastic system. In other words, a larger mechanism should yield greater force and work output concomitantly with greater spring stiffness. Second, homologous structures should serve conserved roles in the functioning of an elastic mechanism such that disabling parts of the system should result in similar effects on the amount of elastic energy storage or the efficiency of the system. Third, a greater kinematic output (e.g., speed and acceleration) should be correlated with a higher spring force, because a more potent spring should provide greater power and work to an elastic system. Here we focus on three questions that revolve around these predictions: (1) Are spring force and spring stiffness correlated with merus length across mantis shrimp or are they decoupled from each other, as has been found in a single-species study of the smasher, *G. falcatus* (Claverie et al., 2011; Zack et al., 2009)? (2) Are the conserved morphologies of the meral-V and saddle across mantis shrimp also reflected in a conserved relative contribution to elastic energy storage? (3) When compared with spearers and undifferentiated species, do the mechanics of the species with faster, hammer-shaped appendages indicate a more robust and powerful spring?

MATERIALS AND METHODS

Animal acquisition and maintenance

Seventy appendages were tested from individuals of twelve mantis shrimp species (Crustacea: Stomatopoda) that were collected from the field using scientific collection permits as appropriate or purchased from aquarium retailers (Table 1). *Hemisquilla californiensis, Lysiosquillina maculata,* and *L. sulcata* individuals were kept in individual 20 L tanks (salinity: 32-36 ppt.; 22°C). *Squilla empusa* individuals were kept in a 341 L tank separated by dividers (salinity: 32-36 ppt.; 14-16 °C). All remaining species were kept in individual 2 L plastic cups, for which the water was changed twice weekly (salinity: 32-36 ppt.; 22°C). Animals were fed a range of fresh and frozen food twice weekly. Data for *G. falcatus* were acquired from a previous publication (Zack et al., 2009).

Mechanical tests

For each animal, body length and mass were measured with digital calipers (Model CD-6"PSX, Mitutoyo Corp., Aurora, IL) and a digital balance (APX-3202, 0.01 g resolution; Dover Instruments, Westborough, MA), respectively. The lateral surface of the merus was photographed 3 times (Nikon D300 SLR camera, AF micro Nikkor 60 mm lens, Nikon, Inc., Melville, NY, U.S.A.). From these pictures, merus length and the maximum span of connective tissue between the meral-V and the main body of the merus were measured and then averaged (Fig. 1) (Sigmascan Pro 5.00, SPSS, Inc, Chicago, IL, U.S.A.). The latter measurement represents the estimated maximum contraction distance of the meral-V, which was used for setting the displacement during the mechanical tests. Appendages were kept wet throughout the preparation to avoid dehydration.

The mechanical tests were conducted as previously described in detail in Zack et al. (2009), thus we will only briefly summarize the preparation here. The mechanical tests were performed by pulling on a wire placed in the same orientation and attached at the site of the extensor muscle to mimic the action of the mantis shrimp loading the spring (materials testing machines: Bluehill 2.12 Instron model 5544; load cell model 2530-416, 0.5 kN maximum, 0.125

N resolution or 0.25 % of load, Instron Corp., Canton, MA, U.S.A. and WaveMatrix 1.4, Instron model E1000; dynamic load cell model 2527-129, 2 kN maximum, resolution of 0.5 % of load, Instron Corp., Canton, MA, U.S.A.). The appendage was compressed to the maximum contraction distance of the meral-V and then relaxed until it returned to its resting position. A velocity was set for each specimen such that the full compression and relaxation phases of the cycle each took 700 ms, the approximate contraction time of the extensor muscle prior to a strike (Burrows and Hoyle, 1972). Force-displacement data were recorded for the compression and relaxation phases at 500 samples per second. Each compression-relaxation cycle was repeated 10 times, waiting at least 3 minutes in between each cycle.

To test the relative contribution of the saddle to elastic energy storage, we severed the saddle on 47 appendages from 40 individuals encompassing 11 species (*Pseudosquilla ciliata* appendages broke within the first 1-2 pulls on intact appendages, so they could not be used for saddle tests). These appendages were contracted 10-20 times with an intact saddle followed by 10 times with the saddle cut by a scalpel along the medial-lateral axis. Given the previous study showing that the number of trials did not affect spring parameters (Zack et al., 2009), we performed a relatively small control study with which to compare the effects of cutting the saddle with tests for which the saddle was not cut. We compared intact saddle tests from trials 11– 20 (one individual was missing trial 11, so we examined trials 12-20 in this case) to intact saddle tests performed from trials 1-10 in 4 species (2 *Gonodactylus chiragra*, 8 *Gonodactylaceus falcatus*, 2 *Gonodactylus smithii*, 1 *Neogonodactylus oerstedii*).

Data analysis

The force-displacement data from the spring tests were used to measure the maximum force of the spring (the maximum force achieved during the force-displacement test), work performed during loading and unloading of the spring (the area under the loading and unloading curves, respectively), resilience (work during unloading divided by work during loading) and the spring constant, *k* (the slope of the force-displacement curve). The spring constant was calculated by fitting linear regressions equal to 25% of the length of the loading curve sequentially along the length of the curve and then finding the line with the peak slope. The first 10% of the force-displacement curve was excluded from this analysis (and all subsequent analyses and calculations) due to spurious noise that often occurred in the first few ms of some tests. A linear curve fit was used, based on alternative model comparisons presented in Zack *et al.* (2009) and also because all of the linear fits in this study were statistically significant (1024 out of 1598 tests had R^2 values exceeding 0.9999; the remainder had R^2 values greater than 0.8933). It should be noted that this method of finding the spring constant differs from previous studies of mantis shrimp in which the spring constant was determined at a set location along the force-displacement curve (Claverie et al., 2011; Zack et al., 2009). We used the dynamic method due to the large variability in the force-displacement curves across taxa and because the fixed location method often missed the location of peak spring constant. Analyses were performed using custom software (Matlab v. 7.11.0, R2010b, The Mathworks, Natick, MA).

The force-displacement data were processed prior to use, due to a programming error in the Instron manufacturer's software that accompanied tests run on the Instron 5544 (Claverie et al., 2011; Zack et al., 2009) in which only the force data were filtered and not the displacement data, causing a temporal offset in the two datasets. Instron engineers provided a Matlab program to fix the problem, which successfully filtered and removed the temporal offset (118 Hz, 4-pole elliptical low pass filter followed by a 10 Hz 2-pole Butterworth low pass filter to the displacement data). The data from *G. falcatus* were originally collected and described in Zack et al. (2009) and re-analyzed using this method as were the rest of the data collected from the Instron model 5544.

Within species, we examined the correlations between merus length and spring characteristics (least-square linear regression), the effect of sex on spring characteristics (Welch two sample t-test), and the effect of cutting the saddle on spring characteristics (Paired two sample t-test) as implemented in R (v. 2.11.1, R_Core_Team, 2012).

Across species, we estimated the degree of phylogenetic signal to be used for phylogenetic tests and applied this scaling parameter (λ) to phylogenetic generalized least squares (PGLS) tests of correlations among appendage type, average species values for spring traits and merus length (ape and caper packages in R, v. 2.15.1, Freckleton et al., 2002; Nunn, 2011; Orme et al., 2012; Paradis et al., 2004; R_Core_Team, 2012). We also examined the association between the effect of cutting the saddle and appendage type. We used two categorizations of appendage type in these analyses. In one set of tests, we coded appendage type as either absence of hammer or presence of hammer. In the second set of tests, we coded appendage type as absence of spear or presence of spear. For all cross-species tests, three datasets were tested: all individuals, males only and females only. Significance level was set at 0.05 and all tests were two-tailed.

We used a recently published molecular phylogeny with branch lengths proportional to genetic change (Porter et al., 2010). The tree was pruned in R to include only the taxa for which we had spring data (Table 1, Fig. 2). We added *Neogonodactylus wennerae* to the *Neogonodactylus* clade as a polytomy based on a previous molecular phylogenetic analysis, which grouped *Neogonodactylus* taxa together (Cheroske et al., 2006).

RESULTS

Scaling of spring mechanics

We compared spring characteristics across species and found that maximum force, work during loading, and work during unloading are significantly correlated with merus length in all datasets (all individuals, males only, females only) (Tables 2-4; Figs. 3-5). Spring constant and resilience show no significant associations with merus length except in the females-only dataset in which resilience is significantly associated with merus length (Tables 3&4; Figs. 4&5). In order to look at scaling within species, we included species for which we had a minimum of 5 individuals, resulting in a total of 4 smasher species and 1 spearer (Table 5). Of the smashers, *G. falcatus*' maximum force, work during loading and unloading are positively correlated with merus length; resilience does not vary with merus length. In *G. smithii*, only work during loading and unloading are positively correlated with merus length. Spring constant scaling is negatively correlated with merus length in two smasher species (*G. chiragra, G. falcatus)* and positively correlated in one spearer species (*L. maculata*).

Of the three species for which we were able to conduct comparisons of males and females (*G. falcatus, G. chiragra, G. smithii*), there are significant differences in spring mechanics and sizes. In terms of the sizes of the appendage components, *G. chiragra* sexes are not significantly different in merus length (t=-0.15, df = 5.4, p=0.89), female merus lengths are larger than males in *G. falcatus* (t=3.44, df=14.1, p=0.004) and smaller in *G. smithii* (t=3.70, df=9.0, p=0.005). The comparisons of spring mechanics only yield differences in *G. falcatus* (all p-values > 0.14 for *G. chiragra* and *G. smithii*). *G. falcatus* males have significantly higher maximum force (Welch two sample t-test, t=3.09, df = 12.3, p=0.009), greater work during loading (t=3.51, df=12.6, p=0.004) and greater work during unloading (t=2.97, df=11.7, p=0.012) than females, even though males have smaller merus lengths than females. Resilience is lower in females than males in *G. falcatus* (t=-2.40, df=13.7, p=0.031) and there is no effect of sex on spring constant (t=-1.04, df=11.2, p=0.32).

Morphological variation and elastic energy storage

Cutting the saddle has no significant effects in the spearer *L. maculata* , but significantly affects all of the spring characteristics in *G. falcatus*, the maximum force, work and resilience in *G. chiragra*, and only force and work in *G. smithii* (Table 6). The decrease in spring function after cutting the saddle is most substantial in work during loading (*G. chiragra*: -20.4%; *G. falcatus*: -18.6%; *G. smithii*: -14.1%), followed by work during unloading (*G. chiragra*: -17.8%; *G. falcatus*: -15.2%; *G. smithii*: -14.0%) and maximum force (*G. chiragra*: -15.6%; *G. falcatus*: -14.5%; *G. smithii*: -10.6%) (Table 6). In the control tests comparing intact saddles at two trial ranges (trials 1-10, 11 or 12-20), we performed paired t-tests by lumping all of the species together and by looking only within *G. falcatus* tests. The results are qualitatively the same for both, so we report only the *G. falcatus* results. Spring constant decreases in the second set of trials (mean difference =-2.47, t = -2.4725, df = 7, p = 0.0427) and the remaining parameters do not change significantly (maximum force: t = -0.8475, df = 7, p = 0.425; work during loading: t = 0.3866, df = 7, p-value = 0.711; work during unloading: t = -0.5384, df = 7, p = 0.607; resilience: t = -2.1227, df = 7, p = 0.0714).

We examined the effect of cutting the saddle in a phylogenetic framework by measuring the percent change in each spring parameter after cutting the saddle and then averaging the individual values to provide a value for each species (Table 7). A greater percent decrease in maximum slope and maximum force occurred in non-hammering shrimp compared to hammering shrimp (maximum slope: t=4.47, p=0.002; maximum force: t=2.70, p=0.027) and in spearing shrimp compared to non-spearing shrimp (maximum slope: t=-3.82, p=0.000; maximum force: t=-2.74, p=0.026). The remaining parameters (percent change after saddle cutting in work loading, work unloading and resilience) are not correlated with appendage type. All tests yield λ = 0, with the exception of maximum slope in the no spear/spear test in which λ =0.856 and is not significantly different from 0 or 1.

During materials testing, the percentages of appendage breakage (defined as when the appendage visibly cracked during the first trial of the test) are 11.6% (n=43 appendages tested) in the smasher species, 72.7% (n=11 appendages) in the undifferentiated species, and 37.5% (n=16 appendages) in the spearer species. The five instances of appendage breakage in smashers occurred at an average of 94% of the total excursion of the meral-V contraction (*G. chiragra:* 94%, 3 individuals; *G. smithii*: 98%, 1 individual; *N. wennerae*: 91%, 1 individual). By contrast, the undifferentiated species and spearer species broke at an average of 74% of the total contraction distance of the meral-V (*H. californiensis*: 66%, 8 individuals; *P. ciliata*: 83%, 6 individuals).

Correlation between spring mechanics and raptorial appendage type

Analyses of the association between spring mechanics and appendage type largely yielded non-significant associations and mixed support for a Brownian motion model of evolution. Work during loading is significantly associated with appendage type by merus length interaction when appendage type is coded as presence and absence of a spear (df=4,6; merus length: t=14.02, p=0.000; appendage type: t=1.09, p=0.317; merus length * appendage type: t=-4.43, p=0.004; λ=1) as is work during unloading (df=4,6; merus length: t=13.7, p=0.000; appendage type: t=0.125, p=0.904; merus length * appendage type: t=-3.43, p=0.014; λ=1) (Figs. 4&5). Similar results were found with resilience, with a significant association with appendage type as well as the interaction term (df=4,6; merus length: t=-0.79, p=0.457; appendage type: t=-5.8, p=0.001; merus length * appendage type: t=4.79, p=0.003; λ=0.96). The remaining spring parameters are not correlated with appendage type. When coded as presence and absence of a hammer, none of the spring features are correlated with appendage type with the exception of resilience (df = 4,6; merus length: t=6.55, p=0.001; appendage type: t=2.67, p=0.037; merus length * appendage type: t=-1.09, p=0.32; λ=1). The results are consistent regardless of whether males and females are combined or analyzed separately.

Given the ambiguities of the ANCOVA results, we also looked at the scaling of spring parameters in the spearers only and the smashers only using PGLS (both analyses leave out the undifferentiated taxon, *Hemisquilla californiensis*) (Table 8). Maximum force and work during unloading are positively correlated with merus length in both analyses. Maximum slope is marginally correlated with merus length in spearers, but not in smashers. Resilience is not correlated with merus length in smashers; the spearer analysis violated the assumptions of the model and thus couldn't be performed.

DISCUSSION

The evolutionary variation of an elastic mechanism revolves around size-scaling, the relative contribution of the mechanism's components to elastic energy storage and the differences in behavioral use or deployment of the mechanism. We find that most elastic features scale predictably with body size across species and that appendage type is associated with several elastic features. Within-species results are not always consistent with the cross-species findings, suggesting that future studies should include both levels of analysis and that large sample sizes are needed to increase the confidence in the interpretation of differing mechanical patterns. The components of the elastic system vary in shape, position and behavior across species, and our results point to possible shifts in function of the saddle and meral-V in the origin of the smasher clade. In the course of the discussion, we critically examine our findings, suggest how the emerging patterns may fit with other spring mechanisms in biology, and briefly discuss future directions for phylogeny-based analyses of spring mechanics.

Are spring force, stiffness and work correlated with merus length?

The within and cross-species results generally show that larger mantis shrimp require more force to compress the elastic mechanism and perform more work during loading and unloading. Spring stiffness does not consistently scale with size within and across species, although within-species scaling is species-specific (Tables 4&5), such that two smasher species have negative size correlations with spring constant and one spearer has a positive size correlation with spring constant (Table 5).

Why would within-species scaling of spring stiffness differ from the lack of association found across species? Although speculative, one possible explanation is that the muscle force required to load the spring scales with body size at a slower rate than inherent exoskeletal stiffness. This would mean that as a spring increases in size, changes in shape or material would be necessary to reduce stiffness scaling such that the muscles could still compress it (Zack et al., 2009). One outcome would be the lack of scaling between spring stiffness and merus size that we found across species (Figs. 4&5). Additionally, if some species use their spring mechanism minimally, or not at all, the muscle-scaling constraint may not be present and thus one would expect spring stiffness and body size to be positively correlated. Indeed, the fact that we see a positive correlation in a spearer (Table 5), which apparently does not flex its meral-V during strikes (deVries et al., In press) and that spearers, in general, are more likely to break during loading (Table 1), suggests that this may be a reasonable hypothesis to test in future studies. Furthermore, in a geometric morphometric analysis of spring shape within and across species, a potential release from selection in the spring of spearers was observed (Claverie and Patek, In revision). At the very least, these results point to the importance of examining spring scaling at both macro-evolutionary scales and within species before ascribing general principles about spring stiffness scaling in muscle-driven systems.

In addition to scaling within and across species, we also find sex differences in one smasher, *G. falcatus*. Even though males have smaller merus length on average than females, their spring force, work and resilience are higher than females. Thus, male *G. falcatus* may have a more robust striking mechanism than do females due to sexual selection or differing sex roles for burrow building or food acquisition (Claverie et al., 2011). *G. falcatus*' dataset, the largest by far, yields the most straightforward scaling findings, suggesting that further studies should include larger datasets and a larger merus length range to effectively tackle within-species scaling issues. Cross-species analyses run with both sexes, males-only or females-only show no substantive differences based on sex.

Another major feature of springs is their resilience – the ability to recover stored elastic energy during unloading. In order to be effective and efficient at releasing energy, the resilience must be high, which is certainly the case in mantis shrimp (overall: 74%; smashers: 76%; spearers: 70%; undifferentiated: 71%). Indeed, even with these overall high levels, smashers have significantly greater resilience than spearers (whether coded as smashers/non-smashers or spearers/non-spearers). It should be noted that resilience measures pose challenges when studying extremely fast release mechanisms. In mantis shrimp, the release of elastic potential energy happens at over 300 times the rate of loading. For example, in *Odontodactylus scyllarus*, the loading of the spring happens on the order of 700 ms and the release occurs in less than 2 ms (Burrows, 1969; Patek et al., 2004; Patek et al., 2007). Even the fastest materials testing machines cannot cycle at these rates, so our estimates of resilience are based on a much slower release of elastic energy than actually occur in the animals. Perhaps different material behavior prevails at very short time scales; to our knowledge, material changes at these time scales have yet to be assessed in any biological system.

The broader applicability of these approaches and findings to other taxa is dependent on the ability to make comparable spring measurements across species. Biological springs follow a consistent behavior during loading: a low slope ("toe region" that represents the slack in the spring) is followed by a linear increase ("plastic region" that equals the maximum rate change in force for a given displacement) and then a transition to a flat slope (Zajac, 1989). While this behavior is repeatable, the displacement of the spring at which the maximum, linear slope occurs is variable. In previous mantis shrimp studies, the slope was measured at a fixed displacement (Claverie et al., 2011; Zack et al., 2009). In the present study, we identify the location dynamically by computationally searching along the length of the force-displacement curve to find the peak slope along the linear region (Fig. 3). We find a negative correlation between merus length and stiffness in *G. falcatus* using the same dataset as used in Claverie et al (Claverie et al., 2011), whereas they found no association with merus length. Formalization of spring measurement approaches is key to successful cross-species analyses of spring mechanics and this dynamic method of identifying the slope may be a first step toward that goal.

Are the conserved spring morphologies reflected in conserved contributions to energy storage?

The overall morphology shows a conserved system in terms of the component parts, but also that the component parts vary noticeably across taxa. All of the species exhibit a prominent saddle that sits on the dorsal or dorsal-medial side of the merus and a meral-V that extends from the lateral meral-carpal joint to a ventral bar that runs along the underside of the merus (Fig. 1).

One notable difference across species is in the placement of the saddle (Fig. 1). In the spearers, the saddle is positioned directly on the dorsal surface of the merus with the midline of the merus approximately running through the midline of the saddle. In contrast, all of the smasher species have a medially located saddle, to the extent that, in some species, the saddle is not visible at all from the lateral side of the merus (Fig. 1). The undifferentiated species, *H. californiensis*, has a slightly medially positioned saddle.

We find that the meral-V is the primary structure used for elastic energy storage across species, yet the appendage is more likely to fracture at an earlier point in its rotation in spearers compared to smashers (Tables 1&2). Indeed, in one spearer species (*P. ciliata*), we were unable to flex the meral-V without appendage fracture. The fracture rates suggest that spearers either do not flex their meral-V's to the extent indicated by their morphology (Fig. 1) or perhaps they use a subtly different loading regime which rotates the meral-V at a different rate or orientation than in the smashers.

Although the saddle does not store the majority of elastic energy, its contributions are substantial. Cutting the saddle decreases spring performance almost uniformly across all species, with the exception of resilience (Table 7). When the saddle is cut, maximum force in the smashers decreases by an average of 15%, spearers by 28% and undifferentiated by 22% (Table 7). Statistical analyses of within-species patterns show significant decreases in spring force and work in three smasher species (Table 6). Cross-species analyses show that spearers exhibit statistically significantly greater decreases in maximum force and spring constant after saddle-cutting compared to smashers.

These results suggest that mantis shrimp are using the elastic components differently across species. The greater fracture rates at smaller excursions of the meral-V in spearers, the generally lower spring work relative to body size in spearers (discussed in next section), and the larger effect of saddle-cutting on spring stiffness and force compared to smashers, suggest that the saddle plays different roles in smashers and spearers. Specifically, stiffness and force can be associated with structural stability and not necessarily elastic energy storage. Thus, the saddle may be functioning to a greater extent for the overall stability and strength of the spearer's merus, while the elastic mechanism, via meral-V flexion, is less potent and less flexible than in smashers. Indeed, this is potentially reflected in the saddle position. The dorsal position of the saddle in spearers is oriented such that it directly opposes the action of the extensor muscle to flex the dorsal exoskeleton of the merus. In contrast, the saddle's more medial orientation in smashers may permit flexion to medial-laterally equilibrate the large, lateral flexions of the meral-V.

Are spring mechanics correlated with raptorial appendage type?

Comparative analyses of spring mechanics between stomatopod taxa with hammers, spears and undifferentiated appendages yield several general results: non-spearers have greater work during loading and greater work during unloading for a given merus length as well as greater resilience compared to spearers (Tables 3&4, Figs. 4&5). Furthermore, when the saddle is cut, spearers experience significantly greater decreases of spring stiffness and maximum spring force. These results are consistent with the findings that spearers strike relatively slowly (deVries et al., In press) and that their spring mechanism is not as robust as in the other mantis shrimp species (Table 1). Thus, as predicted, the fastest mantis shrimp species ("smashers") have more robust springs. The second set of results suggests that the saddle's role has shifted across mantis shrimp species (as discussed above).

If these two lines of evidence are combined with the observation that spearer meral-V's are more likely to fail during loading than in the other species, the overall results suggest that the functions of the spring components have shifted in this clade. Specifically, spearers rely on the saddle for structural support of their raptorial appendages as evidenced by a greater shift in stiffness and maximum force with saddle-severing across species without concomitant effects on the work performed by the system. Given that the smashers are a derived clade, nested within the spearers, it seems likely that their ability to generate extremely fast and powerful strikes is tied to a shift in spring location, function and performance. The final step in these analyses is to more thoroughly probe the basal group, *Hemisquilla* spp., to determine whether they represent a more saddle-based structural system or if they rely more extensively on the meral-V flexion for elastic energy storage.

By comparing spring mechanics within and across species, it is evident that both levels of analysis are necessary to fully understand spring-loading in mantis shrimp. In this case, the within-species comparisons of saddle-cutting suggest that the saddle is more important in smashers than non-smashers. By contrast, the more substantive dataset represented by the cross-species, phylogeny-based analyses, strongly shows an association between saddle-cutting and decrease in maximum force and stiffness in spearers. Thus, this comparative approach shows that a simple “conserved” morphology of an elastic system does not equate with conserved functions/roles of all of the component parts.

Concluding thoughts

Identification of the appropriate morphological or mechanical level at which to compare spring mechanics is a particular challenge of conducting cross-species analyses, given that comparative spring mechanics are pursued from molecular arrangements to the energetics of entire organisms (Bennet-Clark, 1976; Heglund et al., 1982; Tatham and Shewry, 2002). For example, the material composition or molecular arrangements of a spring explain key features like resilience (Burrows et al., 2008; Lv et al., 2010), yet these parameters may not scale up to explain the overall performance or function of the system. Tests of a whole structure – such as a locust or wallaby leg (Katz and Gosline, 1992; McGowan et al., 2008a) – provide mechanical properties that are directly relevant to function, such as if the system operates linearly as a Hookean spring. However, the mechanical properties may not illuminate the material basis for how these spring performance differences are actually achieved, for example, through increases in spring mineralization that increase spring stiffness or spring force. Historically, energetic analyses of movement are most often used to reveal the role of elastic mechanisms (Alexander, 1988; Bennet-Clark, 1976). This approach provides the functional output most closely linked to an organism's performance, but often "black-boxes" the building blocks of the spring mechanism, to the point that the presence of elastic energy storage is known to be vital to the function of the system, but the location of the elastic mechanism is uncertain - the case in many well-studied vertebrate systems (Roberts and Azizi, 2011).

The bulk of mantis shrimp research has focused on the mechanical level of analysis (Claverie et al., 2011; McHenry et al., 2012; Patek et al., 2007; Zack et al., 2009), with fewer analyses of the energetics of the system (Burrows, 1969; McHenry et al., 2012; Patek et al., 2004). The mechanical level has allowed us to test the entire structure such that we approximate and compare the spring-loading regime in the way that the mantis shrimp actually use it. However, the material basis for the variation observed in this study remains unknown. For example, the variable size-stiffness relationships within and across species could be driven by shifts in material composition (e.g., rubbery proteins or mineralization) or solely through shape changes. The saddle's varying contribution to elastic energy storage could be due to material changes or simply the orientation and positioning of the structure. Furthermore, within- and cross-species geometric morphometric analyses of spring shape variation indicate different processes acting at the ontogenetic and macroevolutionary levels (Claverie and Patek, In revision). Reconciling and connecting the biomechanical levels of analysis along with the individual to cross-species levels of analysis offer both challenges and opportunities for probing the sources, patterns and processes involved in the evolutionary history of elastic systems.

With the advent of numerous phylogenies, more tractable phylogeny-based statistical packages and the technical efficiency of mechanical tests, one can hope that this study is at the cusp of a new era in the study of power amplification in organisms – one in which the richness of evolutionary diversity can be used to enhance and inform our understanding of the structure, function and evolution of biological springs.

ACKNOWLEDGEMENTS

R. Caldwell, T. Claverie, M. deVries, D. Drumm, R. Heard, and E. Staaterman made this study possible through their tremendous assistance in locating or collecting mantis shrimp. We are grateful for the advice on phylogenetic comparative methods from C. L. Nunn and for the use of several photographs from R. Caldwell and T. Claverie. T. Claverie, M. deVries, E. Murphy and an anonymous reviewer provided helpful comments on the manuscript. This research was supported by a National Science Foundation (NSF) Minority Postdoctoral Fellowship (to J.R.A.T.), an internship from the Northeast Alliance for Graduate Education and the Professoriate (to M.V.R.), a NSF Integrative Organismal Systems grant (#1014573 to S.N.P.) and a Radcliffe Fellowship (to S.N.P.).

FIGURE LEGENDS

Figure 1. Regardless of appendage type, mantis shrimp share the same basic components of an elastic mechanism found in the merus segment of the raptorial appendages. Spearers, e.g., *Squilla empusa* (A), have an elongate raptorial appendage (B) used for capturing evasive prey. Smashers, e.g., *Gonodactylaceus falcatus* (C), use a hammer-shaped dactyl (D) to smash hard-shelled prey. Undifferentiated taxa, e.g., *Hemisquilla californiensis* (E), use an undifferentiated dactyl (F) to dislodge and process hard-shelled prey (black bar on dactyl is a forcep). A schematic (G) shows an appendage loaded in advance of a strike (left) with the meral-V and saddle compressed through the action of the merus extensor muscles (red dashed line). When released (right), the meral-V and saddle rapidly extend back to their resting state and the meral-V pushes the appendage distally toward the target. When tested in a materials testing machine, a wire was attached and oriented in the same position as the extensor muscle to compress the elastic mechanism similarly to live mantis shrimp. The amount of compression applied by the materials testing machine was determined by the opening between the meral-V and proximal merus (V_{dist}) in the released position. Arrows in animal photos indicate raptorial appendage. Raptorial appendage photos are lateral views of the left appendage. Scale bars are 5 mm. To experience a more detailed perspective of these different appendages types, a supplementary video of rotating, rendered micro-CT scans is available online.

Figure 2. Twelve mantis shrimp species were tested in this study, including an undifferentiated basal species, *H. californiensis* (scale bar = 1 cm), four spearing species (*P. ciliata, L. sulcata, L. maculata* and *S. empusa;* scale bar = 1 cm) and seven smashing species (*G. falcatus, G. chiragra, G. smithii, N. wennerae, N. festae, N. oerstedii, N. bredini*; scale bar = 5 mm). Tree topology and branch lengths (not depicted here) are from the maximum likelihood phylogeny presented in Porter *et al.* (Porter et al., 2010)

with the taxa not tested here pruned from the original tree. *N. wennerae* was added to the tree based on the topology for the genus *Neogonodactylus* in Cheroske *et al* (Cheroske et al., 2006). All of *P. ciliata*'s appendages broke during the tests so those results are not included in the phylogenetic analyses. *N. festae* is placed on this tree for illustrative purposes; it is not included in the phylogenetic analyses, because of the uncertainty in its phylogenetic position. Lateral views of the raptorial appendages are shown.

Figure 3. Representative force displacement curves are shown in each species for which spring compression tests were successfully performed. The thin lines show the displacement from onset of the test to maximum force. The thick lines show the location of maximum slope (spring constant).

Figure 4. The scaling of spring characteristics across species. Each graph shows mean values for each individual within each species using the color-shape scheme shown in the legend.

Figure 5. Cross-species scaling relationships were statistically analyzed using phylogenetic comparative analyses. The values shown here are the means for each species (color-shape scheme in legend) with males and females combined. The lines are calculated using PGLS. Given that these values exhibited $\lambda=0$ (no phylogenetic signal), the lines are equivalent to a regression on the raw data.

Table 1. Sample sizes, collection location, and body sizes of the species used in the study. The rate of appendage failure during materials tests is included; note that all *Pseudosquilla ciliata* failed during material testing. N is the number of individuals and n is the number of appendages tested that did not fail on the first pull. N_t and n_t are the total number of individuals and appendages tested respectively including failures. The appendage failure rate for *G. falcatus* is not reported, because failure data were not comparably recorded in the previous study (Zack et al., 2009). Row colors indicate appendage type (smashers: white; undifferentiated: dark-gray; spearers: light-gray).

Family	**Genus**	**Species**	$N(n)$	$N_t(n_t)$	**Mass (g)**	**Carapace length (mm)**	**Collection location**	**Appendage failure (%)**
Gonodactylidae	*Gonodactylaceus*	*falcatus*	18(18)	--	0.75-3.09	7.92-13.87	Oahu, Hawaii	na
Gonodactylidae	*Gonodactylus*	*chiragra*	13(10)	15(12)	3.00-11.00	12.43-19.39	Lizard Island, Australia	20
Gonodactylidae	*Gonodactylus*	*smithii*	12(11)	15(14)	3.60-6.60	13.84-17.31	Lizard Island, Australia	6.7
Gonodactylidae	*Neogonodactylus*	*bredini*	1(1)	1(1)	1.20	9.51	Isla Galeta, Panama	0
Gonodactylidae	*Neogonodactylus*	*festae*	1(1)	1(1)	1.00	8.58	Isla Naos, Panama	0
Gonodactylidae	*Neogonodactylus*	*oerstedii*	6(6)	7(7)	1.50-4.70	10.28-15.47	Isla Galeta, Panama	0
Gonodactylidae	*Neogonodactylus*	*wennerae*	3(2)	4(3)	2.30-3.70	11.37-13.56	Tampa Bay, Florida	25
Hemisquillidae	*Hemisquilla*	*californiensis*	11(3)	11(3)	29.91-102.21	23.71-35.55	Santa Catalina Island, California	72.7
Lysiosquillidae	*Lysiosquillina*	*maculata*	5(5)	5(5)	36.50-236	27.45-48.42	Lizard Island, Australia	0
Lysiosquillidae	*Lysiosquillina*	*sulcata*	3(3)	3(3)	39.90-50.80	26.94-29.51	Moorea, French Polynesia	0
Pseudosquillidae	*Pseudosquilla*	*ciliata*	4(0)	6(0)	3.81-4.88	14.23-15.23	Oahu, Hawaii	100
Squillidae	*Squilla*	*empusa*	2(2)	2(2)	9.72-20.30	18.84-23.79	Gulf Coast Research Laboratory, Mississippi	0

Table 2. Spring characteristics and size within each species. Results are presented as mean ± standard deviation (minimum – maximum). *one individual was missing body size data. N is the number of individuals tested per species. When two appendages were tested per individual, those two values are averaged to form one value for that individual. Row colors indicate appendage type (smashers: white; undifferentiated: dark-gray; spearers: light-gray).

Species	**N**	**Spring constant (N mm^{-1})**	**Max force (N)**	**Work: load (mJ)**	**Work: unload (mJ)**	**Resilience (%)**	**Body length (mm)**	**Merus length (mm)**
G. falcatus	18	64.78±20.49 (37.43-121.68)	24.87±7.04 (14.38-39.98)	5.32±2.76 (1.89-10.88)	3.88±1.98 (1.29-8.10)	73.51±4.80 (66.55-84.02)	45.28±6.66 (33.34-53.73)	13.76±2.46 (9.32-17.57)
G. chiragra	10*	48.90±18.49 (21.64-80.65)	34.17±6.27 (25.47-43.90)	11.70±4.28 (5.50-16.71)	8.88±4.09 (3.73-14.77)	73.90±10.83 (58.97-88.43)	62.29±8.71 (52.28-82.07)	17.96±2.24 (15.59-22.03)
G. smithii	11	38.80±13.84 (23.12-72.30)	39.84±10.69 (25.23-56.42)	16.81±6.26 (7.85-26.53)	13.16±5.39 (6.08-22.68)	77.92±8.47 (62.25-89.33)	62.11±4.70 (53.88-67.74)	18.45±1.47 (16.24-20.89)
N. bredini	1	27.14	20.08	5.64	4.35	77.26	38.18	12.05
N. festae	1	36.37	18.33	3.87	3.25	84.02	35.51	11.13
N. oerstedii	6	35.62±15.54 (23.56-63.91)	21.85±10.25 (10.01-40.22)	6.47±3.26 (2.07-11.13)	4.55±2.30 (1.11-7.26)	69.15±9.24 (53.55-78.72)	47.49±7.78 (39.14-61.73)	14.06±2.00 (12.50-17.76)
N. wennerae	2	43.33±0.42 (43.03-43.63)	26.77±0.34 (26.53-27.01)	7.58±0.31 (7.36-7.80)	5.75±1.37 (4.78-6.72)	74.77±16.14 (63.36-86.19)	49.93±4.64 (46.65-53.22)	16.01±2.38 (14.32-17.69)
H. californiensis	3	36.21±8.75 (26.80-44.10)	75.75±30.73 (41.38-100.58)	76.48±41.15 (30.18-108.86)	55.14±33.87 (21.30-89.05)	71.24±10.36 (61.20-81.89)	147.69±27.37 (118.97-173.47)	30.34±6.81 (22.74-35.90)
L. maculata	5	46.67±16.03 (24.38-62.81)	87.31±35.98 (37.38-125.24)	60.01±31.58 (20.57-96.48)	49.34±26.17 (16.18-82.51)	82.37±4.91 (78.35-89.44)	225.81±47.13 (147.03-266.71)	43.54±10.45 (26.56-54.37)
L. sulcata	3	45.12±5.50 (38.86-49.20)	31.99±11.53 (21.34-44.24)	9.673±4.56 (6.00-26.53)	7.01±3.75 (3.84-11.16)	70.97±6.13 (64.02-75.58)	158.13±8.56 (152.01-167.91)	28.63±3.45 (24.94-31.77)
S. empusa	2	37.63±2.04 (36.18-39.07)	28.57±4.82 (25.16-31.98)	9.74±3.29 (7.42-12.06)	5.72±2.49 (3.96-7.48)	57.73±5.98 (53.50-61.96)	97.41±15.24 (86.63-108.18)	21.16±3.87 (18.43-23.90)

Table 3. The ratios of spring parameters to merus length (ML) across species. Results are presented as mean ± standard deviation. *one individual was missing body size data. N is the number of individuals tested per species. When two appendages were tested per individual, those two values are averaged to form one value for that individual. Row colors indicate appendage type (smashers: white; undifferentiated: dark-gray; spearers: light-gray).

Species	**N**	**Spring constant/ML ($N\ mm^{-1}$)**	**Max force/ML ($N\ mm^{-1}$)**	**Work: load/ML ($mJ\ mm^{-1}$)**	**Work: unload/ML ($mJ\ mm^{-1}$)**	**Resilience/ML ($\%\ mm^{-1}$)**
G. falcatus	18	5.02±2.46	1.80±0.35	0.37±0.14	0.27±0.10	5.51±1.05
G. chiragra	10*	2.90±1.34	1.94±0.46	0.64±0.23	0.49±0.22	4.15±0.64
G. smithii	11	2.13±0.81	2.15±0.54	0.90±0.30	0.70±0.25	4.24±0.50
N. bredini	1	2.25	1.67	0.47	0.36	6.41
N. festae	1	3.27	1.65	0.35	0.29	7.55
N. oerstedii	6	2.63±1.33	1.60±0.85	0.47±0.25	0.33±0.17	4.97±0.77
N. wennerae	2	2.74±0.43	1.69±0.23	0.48±0.05	0.36±0.03	4.65±0.32
H. californiensis	3	1.20±0.16	2.42±0.53	2.38±0.92	1.71±0.77	2.43±0.62
L. maculata	5	1.05±0.16	1.94±0.51	1.31±0.52	1.08±0.44	2.00±0.58
L. sulcata	3	1.60±0.34	1.14±0.43	0.34±0.16	0.25±0.13	2.52±0.47
S. empusa	2	1.82±0.43	1.35±0.02	0.45±0.07	0.26±0.07	2.75±0.22

Table 4. The relationships between merus length as the independent variable and spring characteristics as the dependent variables across species, calculated using Phylogenetic Generalized Least Squares with mean species values. The statistical results apply to the coefficient. None of the intercepts are significantly different from zero, except for resilience (t=13.043, p=0.0000). Statistically significant values are indicated in bold. The results of using the combined males and females dataset are presented here; males only and females only datasets yield qualitatively similar results with the exception of resilience in females (λ =1 ; intercept: 60.7; coeff.: 0.71; std.err.: 0.15; p=0.0045). λ represents phylogenetic correlation ranging from 0 (no phylogenetic signal) to 1 (Brownian motion) (Freckleton et al., 2002; Pagel, 1999). λ is 0 for the data shown here.

	Intercept	**Coefficient**	**Standard error**	**t-value**	**P-value**
Spring constant (N mm^{-1})	37.93	0.17	0.39	0.4403	0.6713
Maximum force (N)	**-6.17**	**2.09**	**0.36**	**5.8498**	**0.0004**
Work: load (mJ)	**-21.69**	**1.97**	**0.53**	**3.6819**	**0.0062**
Work: unload (mJ)	**-17.87**	**1.56**	**0.39**	**4.0265**	**0.0038**
Resilience (%)	70.68	0.11	0.24	0.4758	0.6470

Table 5. The scaling of spring characteristics relative to merus length within each species using a least-squares linear regression. Statistically significant values are indicated in bold. *L. maculata* (gray) is a spearer; the remaining species are smashers.

	Species	**Intercept**	**Slope**	**F-statistic**	**df**	**P-value**	**R^2**
Spring constant ($N\ mm^{-1}$)	***falcatus***	**121.35**	**-4.11**	**5.14**	**1,16**	**0.0376**	**0.2431**
	chiragra	**176.66**	**-7.07**	**13.74**	**1,7**	**0.0076**	**0.6625**
	smithii	88.33	-2.68	0.79	1,9	0.3960	0.0811
	oerstedii	84.73	-3.49	1.01	1,4	0.3713	0.2019
	maculata	**-15.68**	**1.43**	**20.24**	**1,3**	**0.0205**	**0.8709**
Maximum force (N)	***falcatus***	**-4.37**	**2.12**	**19.59**	**1,16**	**0.0004**	**0.5504**
	chiragra	41.92	-0.42	0.15	1,7	0.7134	0.0205
	smithii	-24.45	3.48	2.67	1,9	0.1364	0.2291
	oerstedii	38.90	-1.21	0.24	1,4	0.6517	0.0560
	maculata	-41.03	2.95	8.23	1,3	0.0642	0.7327
Work: load (mJ)	***falcatus***	**-7.90**	**0.96**	**43.27**	**1,16**	**0.0000**	**0.7301**
	chiragra	-9.71	1.19	3.69	1,7	0.0964	0.3449
	smithii	**-35.54**	**2.84**	**7.16**	**1,9**	**0.0254**	**0.4429**
	oerstedii	6.92	-0.03	0.00	1,4	0.9708	0.0004
	maculata	-47.59	2.47	6.05	1,3	0.0908	0.6686
Work: unload (mJ)	***falcatus***	**-5.58**	**0.69**	**43.45**	**1,16**	**0.0000**	**0.7309**
	chiragra	-12.17	1.17	4.06	1,7	0.0836	0.3673
	smithii	**-34.76**	**2.60**	**9.00**	**1,9**	**0.0150**	**0.4999**
	oerstedii	2.56	0.14	0.06	1,4	0.8162	0.0152
	maculata	-38.09	2.01	5.39	1,3	0.1028	0.6426
Resilience (%)	*falcatus*	73.27	0.02	0.00	1,16	0.9713	0.0001
	chiragra	34.19	2.22	1.61	1,7	0.2446	0.1873
	smithii	52.04	1.40	0.57	1,9	0.4712	0.0591
	oerstedii	46.73	1.60	0.54	1,4	0.5028	0.1191
	maculata	79.92	0.06	0.04	1,3	0.8479	0.0143

Table 6. The effects of cutting the saddle on spring characteristics across species. Paired t-tests were performed, except when data were not normally distributed. *In this latter case, a paired Wilcoxon signed rank test was performed (indicated by "V=") in the t-value column. Statistically significant values are indicated in bold. *L. maculata* is a spearer (gray); the remaining species are smashers.

	Species	t-value*	df	P-value	Mean of differences
Spring constant (N mm^{-1})	***falcatus***	**4.2373**	**13**	**0.0010**	**4.45**
	chiragra	0.6211	9	0.5499	1.07
	smithii	-1.2008	10	0.2575	-1.18
	oerstedii	1.3386	5	0.2383	8.01
	maculata	-1.7609	3	0.1765	-14.25
Maximum force (N)	***falcatus***	**8.0989**	**13**	**0.0000**	**3.60**
	chiragra	**6.1219**	**9**	**0.0002**	**5.31**
	smithii	**V = 61**		**0.0098**	**4.23**
	oerstedii	1.7444	5	0.1415	6.46
	maculata	V = 1		0.2500	-32.05
Work: load (mJ)	***falcatus***	**5.6182**	**13**	**0.0001**	**0.99**
	chiragra	**4.6379**	**9**	**0.0012**	**2.38**
	smithii	**3.413**	**10**	**0.0066**	**2.37**
	oerstedii	1.9583	5	0.1075	1.96
	maculata	-2.1381	3	0.1221	-21.75
Work: unload (mJ)	***falcatus***	**4.5751**	**13**	**0.0005**	**0.59**
	chiragra	**4.0228**	**9**	**0.0030**	**1.58**
	smithii	**2.9778**	**10**	**0.0139**	**1.84**
	oerstedii	1.8299	5	0.1268	1.24
	maculata	-2.0155	3	0.1372	-18.06
Resilience (%)	***falcatus***	**-3.7337**	**13**	**0.0025**	**-2.57**
	chiragra	**-3.2098**	**9**	**0.0107**	**-1.98**
	smithii	-0.3516	10	0.7324	-0.53
	oerstedii	-1.8154	5	0.1292	-2.79
	maculata	0.2508	3	0.8182	0.37

Table 7. Percent change in spring parameter after the saddle was severed; negative values indicate a decrease after the saddle was cut. Individual values were calculated and then averaged to generate species means. Row colors indicate appendage type (smashers: white; undifferentiated: dark-gray; spearers: light-gray).

Species	**n**	**Spring constant**	**Maximum force**	**Work: load**	**Work: unload**	**Resilience**
falcatus	14	-6.5	-13.4	-15.8	-12.7	3.6
chiragra	9	-0.4	-16.4	-21.3	-19.4	2.5
smithii	11	4.0	-10.0	-13.3	-12.6	0.8
bredini	1	-3.2	-23.1	-27.5	-27.0	0.5
festae	1	6.0	-15.8	-21.0	-22.4	-1.7
oerstedii	6	-13.5	-21.8	-24.3	-20.1	4.6
wennerae	2	-15.5	-7.7	-0.7	8.4	8.9
californiensis	1	-17.1	-21.5	-21.0	-18.9	2.6
maculata	4	-27.7	-35.0	-34.7	-34.3	0.5
sulcata	1	-38.6	-20.3	-1.3	-1.5	-0.4
empusa	2	-33.5	-30.1	-28.1	-19.5	11.7

Table 8. The scaling of spring characteristics relative to merus length in two different datasets - one including only species with spears and the other consisting of species with hammers. The analyses were calculated using Phylogenetic Generalized Least Squares with mean species values. The statistical results apply to the coefficient. None of the intercepts are significantly different from zero, except for the spring constant in spearers (t=6.23, p=0.0248) and resilience in species with hammers (t=8.08, p=0.0013). **λ** represents phylogenetic correlation ranging from 0 (no phylogenetic signal) to 1 (Brownian motion) (Freckleton et al., 2002; Pagel, 1999). Assumptions were violated for the resilience calculation in spearers, so those values are not included. Row colors indicate appendage type (smashers: white; spearers: light-gray). Statistically significant values are indicated in bold.

	Intercept	**Coefficient**	**Standard error**	**t-value**	**P-value**	**λ**
Spring constant (N mm^{-1})	33.23	0.51	1.98	0.26	0.8083	1
	27.47	0.40	0.09	4.26	0.0509	1
Maximum force (N)	**-14.58**	**2.77**	**0.46**	**6.01**	**0.0039**	**0**
	-18.58	**2.65**	**0.37**	**7.07**	**0.0194**	**1**
Work: load (mJ)	**-13.78**	**1.48**	**0.40**	**3.73**	**0.0203**	**0**
	-16.28	2.27	0.58	3.89	0.0602	1
Work: unload (mJ)	**-11.16**	**1.17**	**0.33**	**3.52**	**0.0244**	**0**
	-21.36	**1.97**	**0.42**	**4.73**	**0.0419**	**1**
Resilience (%)	72.94	0.11	0.59	0.19	0.8574	0
	na	na	na	na	na	na

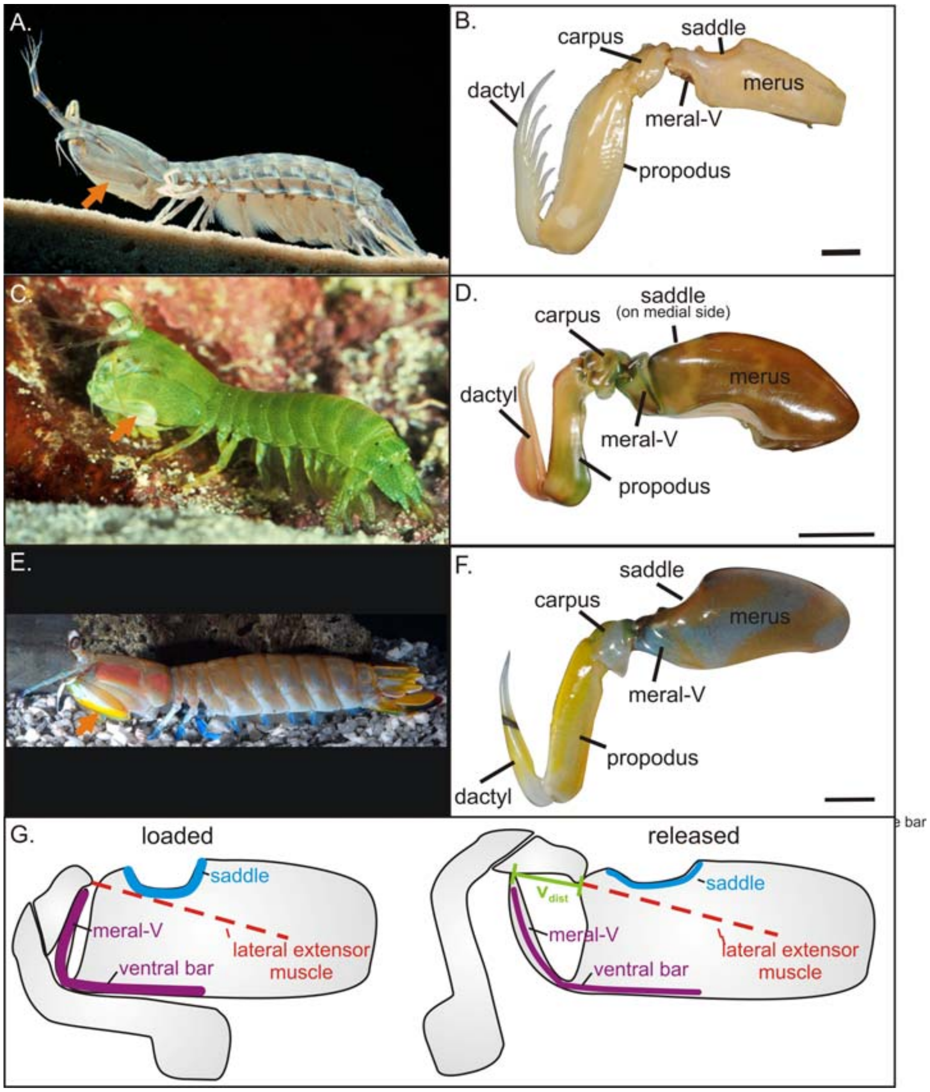

Figure 1. Regardless of appendage type, mantis shrimp share the same basic components of an elastic mechanism found in the merus segment of the raptorial appendages. Spearers, e.g., *Squilla empusa* (A), have an elongate raptorial appendage (B) used for capturing evasive prey. Smashers, e.g., *Gonodactylaceus falcatus* (C), use a hammer-shaped dactyl (D) to smash hard-shelled prey. Undifferentiated taxa, e.g., *Hemisquilla californiensis* (E), use an undifferentiated dactyl (F) to dislodge and process hard-shelled prey (black bar on dactyl is a forcep). A schematic (G) shows an appendage loaded in advance of a strike (left) with the meral-V and saddle compressed through the action of the merus extensor muscles (red dashed line). When released (right), the meral-V and saddle rapidly extend back to their resting state and the meral-V pushes the appendage distally toward the target. When tested in a materials testing machine, a wire was attached and oriented in the same position as the extensor muscle to compress the elastic mechanism similarly to live mantis shrimp. The amount of compression applied by the materials testing machine was determined by the opening between the meral-V and proximal merus (V_{dist}) in the released position. Arrows in animal photos indicate raptorial appendage. Raptorial appendage photos are lateral views of the left appendage. Scale bars are 5 mm. To experience a more detailed perspective of these different appendages types, a supplementary video of rotating, rendered micro-CT scans is available online.

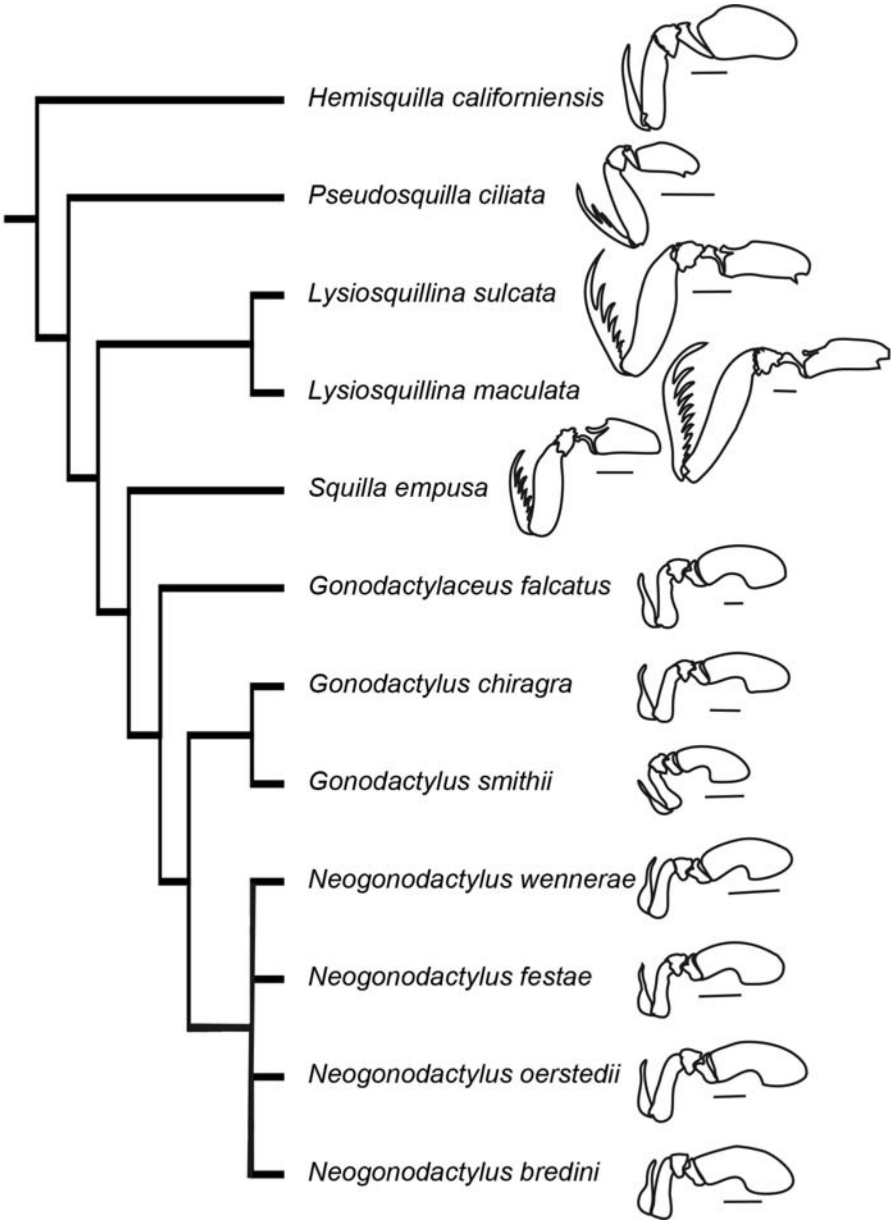

Figure 2. Twelve mantis shrimp species were tested in this study, including an undifferentiated basal species, *H. californiensis* (scale bar = 1 cm), four spearing species (*P. ciliata, L. sulcata, L. maculata* and *S. empusa;* scale bar = 1 cm) and seven smashing species (*G. falcatus, G. chiragra, G. smithii, N. wennerae, N. festae, N. oerstedii, N. bredini*; scale bar = 5 mm). Tree topology and branch lengths (not depicted here) are from the maximum likelihood phylogeny presented in Porter *et al.* (Porter et al., 2010) with the taxa not tested here pruned from the original tree. *N. wennerae* was added to the tree based on the topology for the genus *Neogonodactylus* in Cheroske *et al* (Cheroske et al., 2006). All of *P. ciliata*'s appendages broke during the tests so those results are not included in the phylogenetic analyses. *N. festae* is placed on this tree for illustrative purposes; it is not included in the phylogenetic analyses, because of the uncertainty in its phylogenetic position. Lateral views of the raptorial appendages are shown.

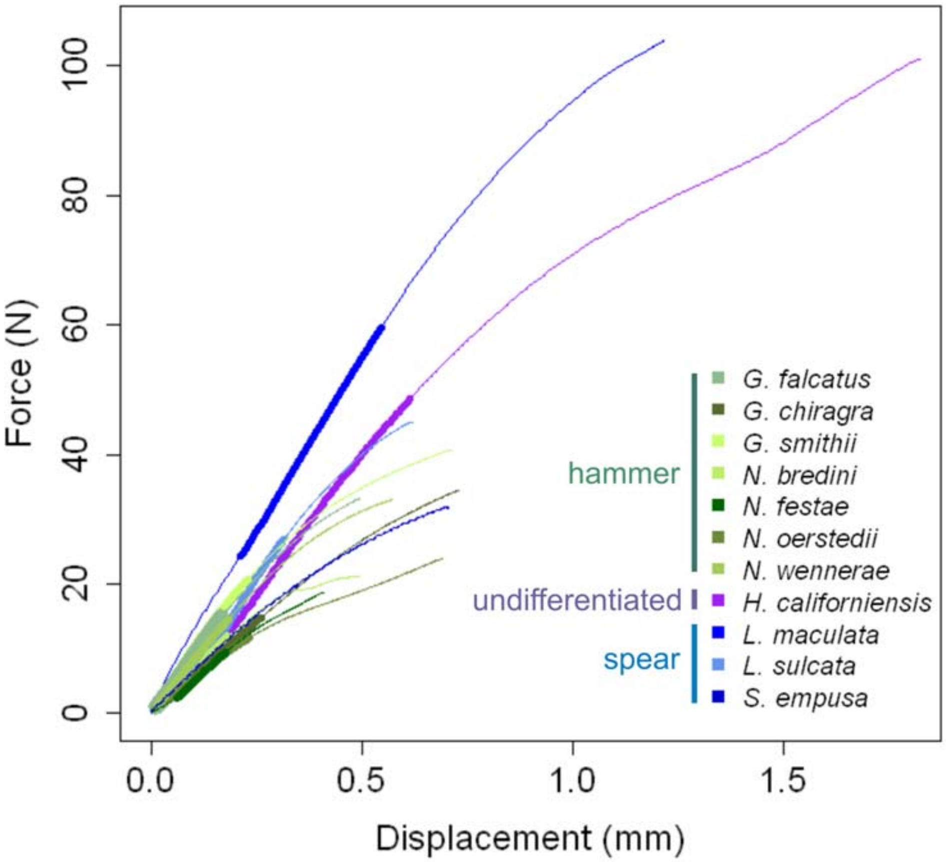

Figure 3. Representative force displacement curves are shown in each species for which spring compression tests were successfully performed. The thin lines show the displacement from onset of the test to maximum force. The thick lines show the location of maximum slope (spring constant).

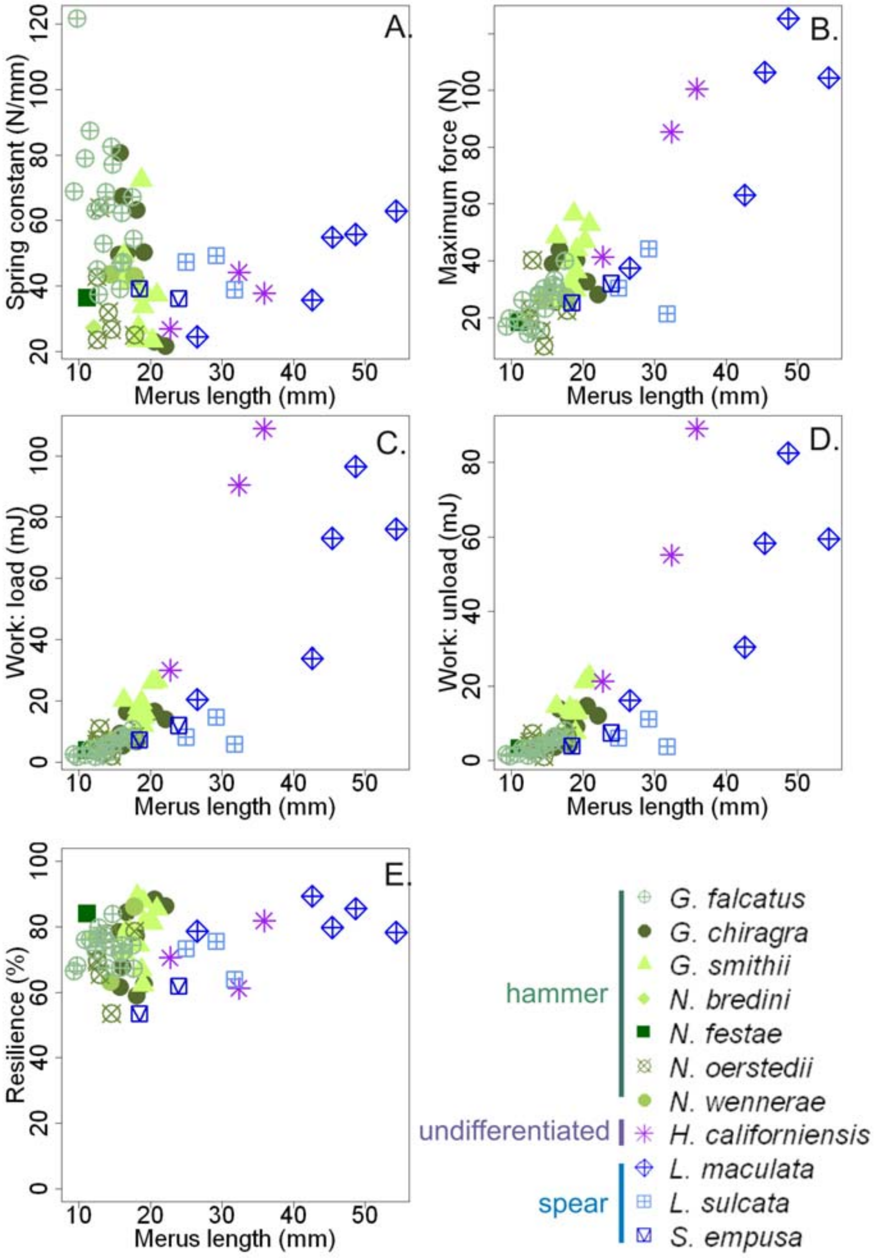

Figure 4. The scaling of spring characteristics across species. Each graph shows mean values for each individual within each species using the color-shape scheme shown in the legend.

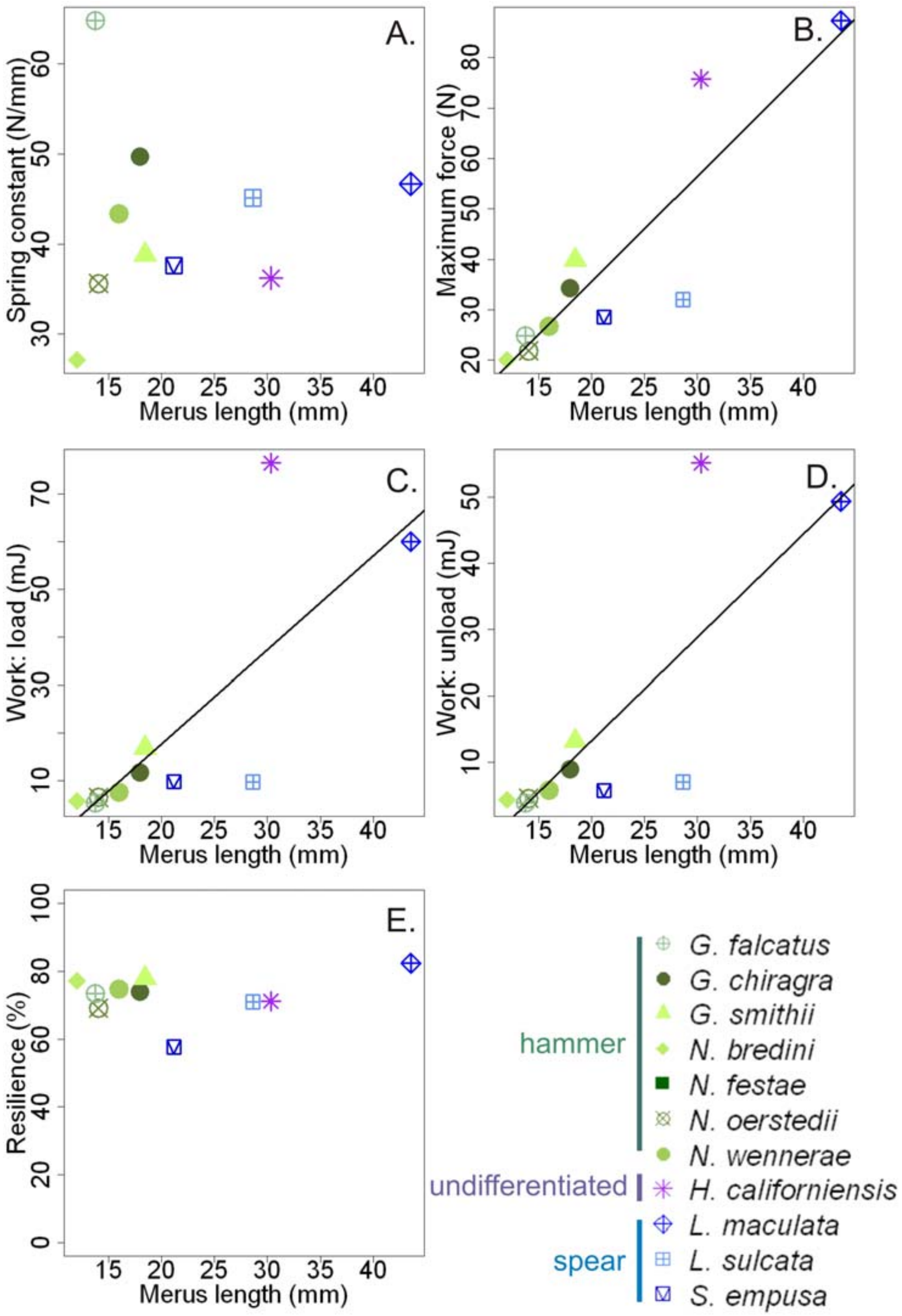

Figure 5. Cross-species scaling relationships were statistically analyzed using phylogenetic comparative analyses. The values shown here are the means for each species (color-shape scheme in legend) with males and females combined. The lines are calculated using PGLS. Given that these values exhibited λ=0 (no phylogenetic signal), the lines are equivalent to a regression on the raw data.

REFERENCES CITED

Ahyong, S. T. (2001). Revision of the Australian Stomatopod Crustacea. Sydney: Australian Museum.

Ahyong, S. T. and Harling, C. (2000). The phylogeny of the stomatopod Crustacea. *Australian Journal of Zoology* **48**, 607-642.

Ahyong, S. T. and Jarman, S. N. (2009). Stomatopod interrelationships: preliminary results based on analysis of three molecular loci. *Arthropod Systematics & Phylogeny* **67**, 91-98.

Alexander, R. M. (1988). Elastic mechanisms in animal movement. New York: Cambridge University Press.

Alexander, R. M. (2003). Principles of animal locomotion. Princeton: Princeton University Press.

Alexander, R. M. and Vernon, A. (1975). The mechanics of hopping by kangaroos (Macropodidae). *Journal of Zoology, London* **177**, 265-303.

Bachmann, T., Emmerlich, J., Baumgartner, W., Schneider, J. M. and Wagner, H. (2012). Flexural stiffness of feather shafts: geometry rules over material properties. *The Journal of Experimental Biology* **215**, 405-415.

Bennet-Clark, H. C. (1976). Energy storage in jumping insects. In *The Insect Integument*, (ed. H. R. Hepburn), pp. 421-443. Amsterdam: Elsevier Scientific Publishing Company.

Burrows, M. (1969). The mechanics and neural control of the prey capture strike in the mantid shrimps *Squilla* and *Hemisquilla*. *Zeitschrift für vergleichende Physiologie* **62**, 361-381.

Burrows, M. and Hoyle, G. (1972). Neuromuscular physiology of the strike mechanism of the mantis shrimp, *Hemisquilla*. *Journal of Experimental Zoology* **179**, 379-394.

Burrows, M., Shaw, S. and Sutton, G. (2008). Resilin and chitinous cuticle form a composite structure for energy storage in jumping by froghopper insects. *BMC Biology* **6**, 41.

Caldwell, R. L. (1975). Ecology and evolution of agonistic behavior in Stomatopods. *Naturwissenschaften* **62**, 214-222.

Caldwell, R. L. and Dingle, H. (1976). Stomatopods. *Scientific American*, 81-89.

Cheroske, A. G., Barber, P. H. and Cronin, T. W. (2006). Evolutionary variation in the expression of phenotypically plastic color vision in Caribbean mantis shrimps, genus *Neogonodactylus*. *Marine Biology* **150**, 213-220.

Claverie, T., Chan, E. and Patek, S. N. (2011). Modularity and scaling in fast movements: power amplification in mantis shrimp. *Evolution* **62**, 443-461.

Claverie, T. and Patek, S. N. (In revision). Correlated evolution and evolutionary disparity of the power-amplified system in mantis shrimp *Evolution*.

deVries, M. S., Murphy, E. A. K. and Patek, S. N. (In press). Strike mechanics of an ambush predator: the spearing mantis shrimp. *Journal of Experimental Biology*.

Freckleton, R. P., Harvey, P. H. and Pagel, M. (2002). Phylogenetic analysis and comparative data: A test and review of evidence. *The American Naturalist* **160**, 712-726.

Hayashi, M., Feilich, K. L. and Ellerby, D. J. (2009). The mechanics of explosive seed dispersal in orange jewelweed (*Impatiens capensis*). *Journal of Experimenal Botany* **60**, 2045-2053.

Hayashi, M., Gerry, S. P. and Ellerby, D. J. (2010). The seed dispersal catapult of *Cardamine parviflora* (Brassicaceae) is efficient but unreliable. *American Journal of Botany* **97**, 1595-1601.

Heglund, N., Fedak, M., Taylor, C. and Cavagna, G. (1982). Energetics and mechanics of terrestrial locomotion. IV. Total mechanical energy changes as a function of speed and body size in birds and mammals. *Journal of Experimental Biology* **97**, 57-66.

Katz, S. L. and Gosline, J. M. (1992). Ontogenetic scaling and mechanical behaviour of the tibiae of the African desert locust (*Schistocerca gregaria*). *Journal of Experimental Biology* **168**, 125-150.

Lohse, D., Schmitz, B. and Versluis, M. (2001). Snapping shrimp make flashing bubbles. *Nature* **413**, 477-478.

Lv, S., Dudek, D. M., Cao, Y., Balamurali, M. M., Gosline, J. and Li, H. B. (2010). Designed biomaterials to mimic the mechanical properties of muscles. *Nature* **465**, 69-73.

McGowan, C. P., Baudinette, R. V. and Biewener, A. A. (2008a). Differential design for hopping in two species of wallabies. *Comparative Biochemistry and Physiology - Part A: Molecular & Integrative Physiology* **150**, 151-158.

McGowan, C. P., Skinner, J. and Biewener, A. A. (2008b). Hind limb scaling of kangaroos and wallabies (superfamily Macropodoidea): implications for hopping performance, safety factor and elastic savings. *Journal of Anatomy* **212**, 153-163.

McHenry, M. J., Claverie, T., Rosario, M. V. and Patek, S. N. (2012). Gearing for speed slows the predatory strike of a mantis shrimp. *Journal of Experimental Biology* **215**, 1231-1245.

McNeill, P., Burrows, M. and Hoyle, G. (1972). Fine structures of muscles controlling the strike of the mantis shrimp, *Hemisquilla*. *Journal of Experimental Zoology* **179**, 395-416.

Nüchter, T., Benoit, M., Engel, U., Özbek, S. and Holstein, T. W. (2006). Nanosecond-scale kinetics of nematocyst discharge. *Current Biology* **16**, R316-R318.

Nunn, C. L. (2011). The Comparative Approach in Evolutionary Anthropology and Biology. Chicago: The University of Chicago Press.

Orme, D., Freckleton, R., Thomas, G., Petzoldt, T., Fritz, S., Isaac, N. and Pearse, W. (2012). caper: Comparative Analyses of Phylogenetics and Evolution in R. In *R*.

Pagel, M. (1999). Inferring the historical patterns of biological evolution. *Nature* **401**, 877-884.

Paradis, E., Claude, J. and Strimmer, K. (2004). APE: analyses of phylogenetics and evolution in R. *Bioinformatics* **20**, 289-290.

Patek, S. N., Baio, J. E., Fisher, B. F. and Suarez, A. V. (2006). Multifunctionality and mechanical origins: ballistic jaw propulsion in trap-jaw ants. *Proceedings of the National Academy of Sciences* **103**, 12787-12792.

Patek, S. N. and Caldwell, R. L. (2005). Extreme impact and cavitation forces of a biological hammer: strike forces of the peacock mantis shrimp (*Odontodactylus scyllarus*). *Journal of Experimental Biology* **208**, 3655-3664.

Patek, S. N., Dudek, D. M. and Rosario, M. V. (2011). From bouncy legs to poisoned arrows: elastic movements in invertebrates. *The Journal of Experimental Biology* **214**, 1973-1980.

Patek, S. N., Korff, W. L. and Caldwell, R. L. (2004). Deadly strike mechanism of a mantis shrimp. *Nature* **428**, 819-820.

Patek, S. N., Nowroozi, B. N., Baio, J. E., Caldwell, R. L. and Summers, A. P. (2007). Linkage mechanics and power amplification of the mantis shrimp's strike. *Journal of Experimental Biology* **210**, 3677 - 3688.

Porter, M. L., Zhang, Y., Desai, S., Caldwell, R. L. and Cronin, T. W. (2010). Evolution of anatomical and physiological specialization in the compound eyes of stomatopod crustaceans. *Journal of Experimental Biology* **213**, 3473-3486.

R_Core_Team. (2012). R: A language and environment for statistical computing. Vienna, Austria: R Foundation for Statistical Computing.

Roberts, T. J. and Azizi, E. (2011). Flexible mechanisms: the diverse roles of biological springs in vertebrate movement. *Journal of Experimental Biology* **214**, 353-361.

Schram, F. R. (2007). Paleozoic proto-mantis shrimp revisited. *Journal of Paleontology* **81**, 895-916.

Seid, M. A., Scheffrahn, R. H. and Niven, J. E. (2009). The rapid mandible strike of a termite soldier. *Current Biology* **18**, R1049-R1050.

Sensenig, A. T. and Schultz, J. W. (2004). Elastic energy storage in the pedipalpal joints of scorpions and sun-spiders (Arachnida, Scorpiones, Solifugae). *Journal of Arachnology* **32**, 1-10.

Sensenig, A. T. and Shultz, J. W. (2003). Mechanics of cuticular elastic energy storage in leg joints lacking extensor muscles in arachnids. *Journal of Experimental Biology* **206**, 771-784.

Spagna, J. C., Vakis, A. I., Schmidt, C. A., Patek, S. N., Zhang, X., Tsutsui, N. D. and Suarez, A. V. (2008). Phylogeny, scaling, and the generation of extreme forces in trap-jaw ants. *Journal of Experimental Biology* **211**, 2358-2368.

Tatham, A. S. and Shewry, P. R. (2002). Comparative structures and properties of elastic proteins. *Philosphical Transactions of the Royal Society London B* **357**, 229-234.

Versluis, M., Schmitz, B., von der Heydt, A. and Lohse, D. (2000). How snapping shrimp snap: through cavitating bubbles. *Science* **289**, 2114-2117.

Vogel, S. (2005). Living in a physical world III. Getting up to speed. *Journal of Biosciences* **30**, 303-312.

Wainwright, S. A., Biggs, W. D., Currey, J. D. and Gosline, J. M. (1976). Mechanical design in organisms. Princeton: Princeton University Press.

Weaver, J. C., Milliron, G. W., Miserez, A., Evans-Lutterodt, K., Herrera, S., Gallana, I., Mershon, W. J., Swanson, B., Zavattieri, P., DiMasi, E. et al. (2012). The stomatopod dactyl club: a formidable damage-tolerant biological hammer. *Science* **336**, 1275-1280.

Zack, T. I., Claverie, T. and Patek, S. N. (2009). Elastic energy storage in the mantis shrimp's fast predatory strike. *Journal of Experimental Biology* **212**, 4002-4009.

Zajac, F. E. (1989). Muscle and tendon: properties, models, scaling, and application to biomechanics and motor control. *Critical Reviews in Biomedical Engineering* **17**, 359 - 411.

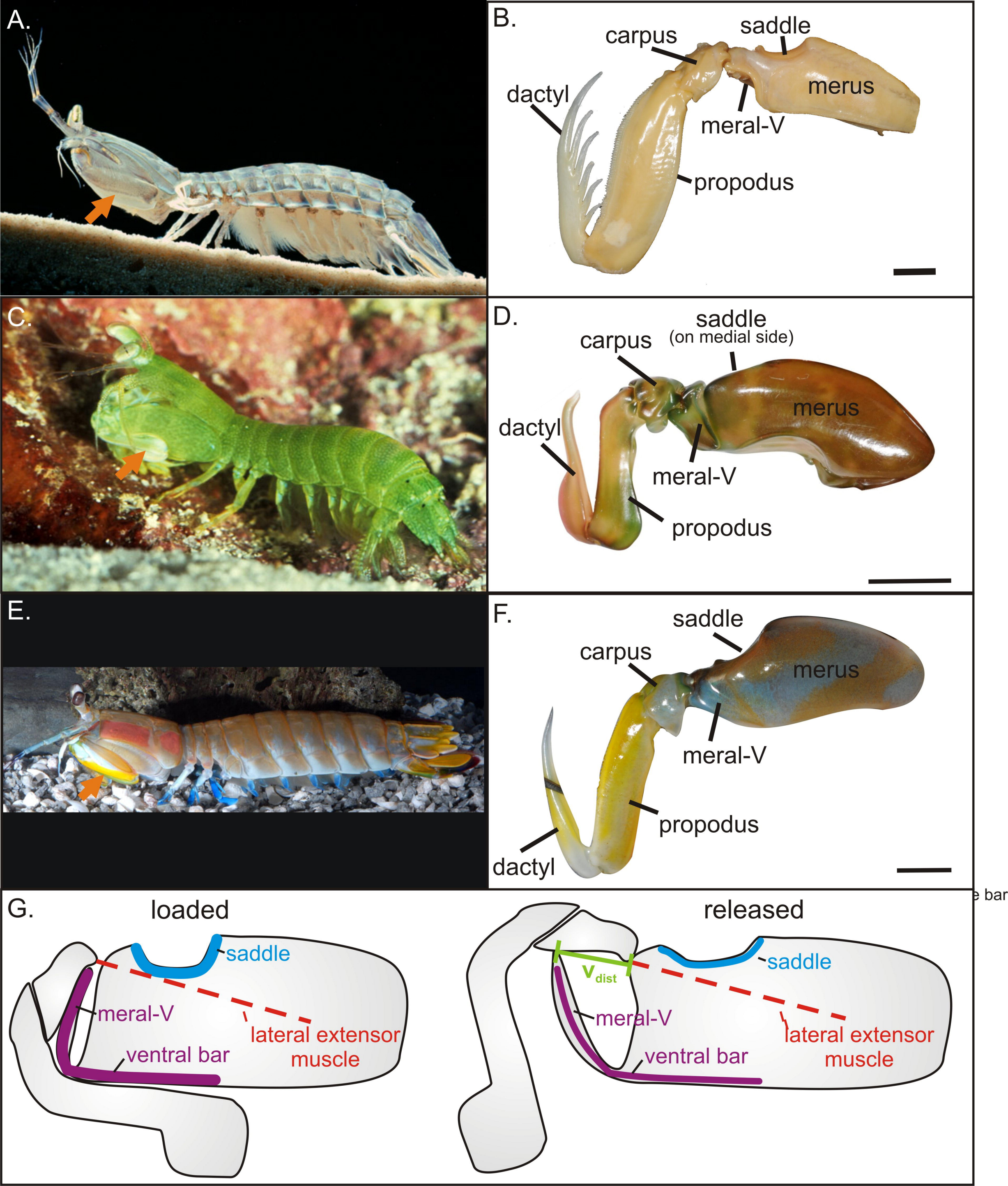
A.
B.
carpus
saddle
dactyl
merus
meral-V
propodus
C.
D.
saddle
(on medial side)
carpus
dactyl
merus
meral-V
propodus
E.
F.
saddle
carpus
merus
meral-V
propodus
dactyl
e bar
G.
loaded
saddle
meral-V
lateral extensor
muscle
ventral bar
released
saddle
V_{dist}
meral-V
lateral extensor
muscle
ventral bar

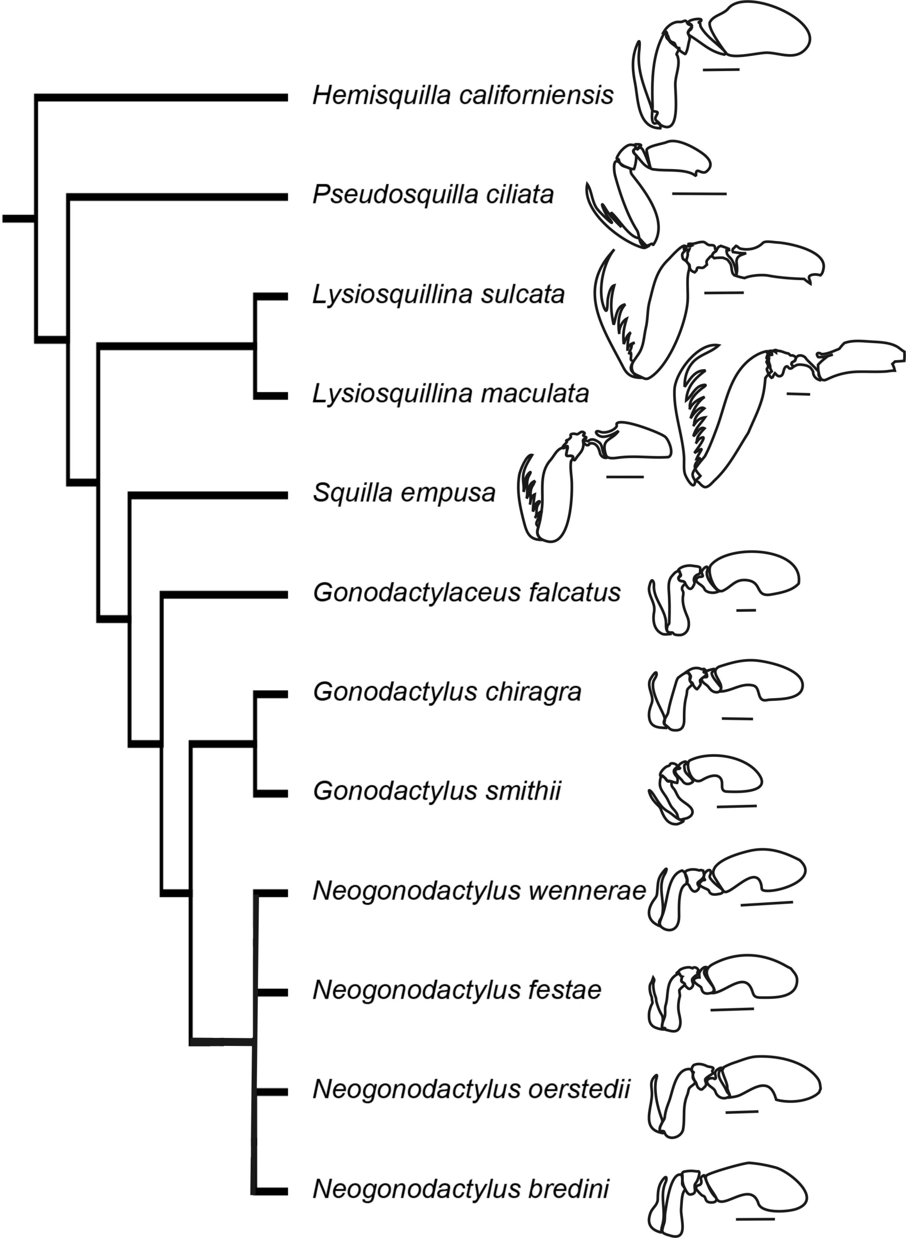
Hemisquilla californiensis
Pseudosquilla ciliata
Lysiosquillina sulcata
Lysiosquillina maculata
Squilla empusa
Gonodactylaceus falcatus
Gonodactylus chiragra
Gonodactylus smithii
Neogonodactylus wennerae
Neogonodactylus festae
Neogonodactylus oerstedii
Neogonodactylus bredini

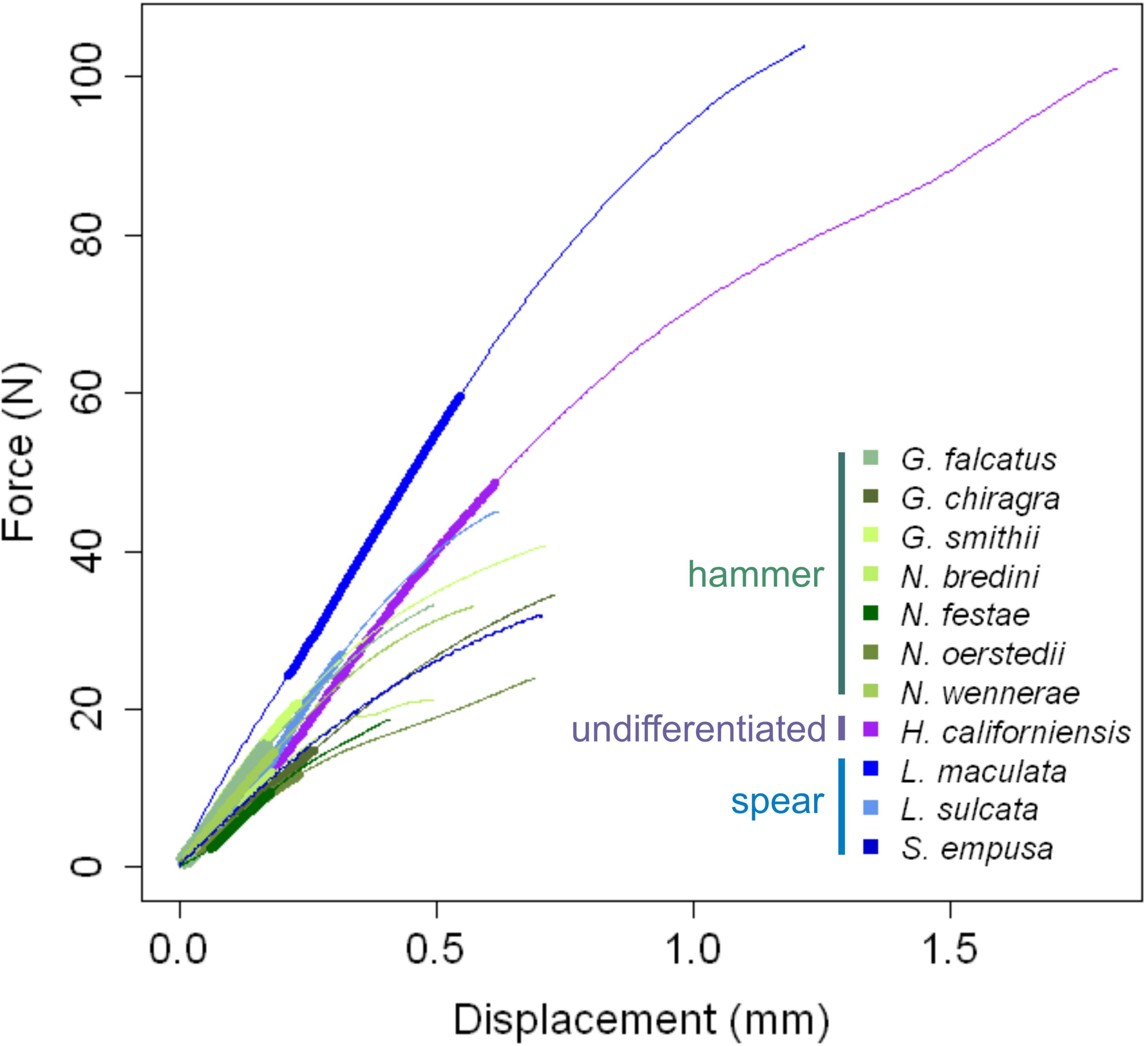
Force (N)
0
20
40
60
80
100
Displacement (mm)
0.0
0.5
1.0
1.5
hammer
undifferentiated
spear
G. falcatus
G. chiragra
G. smithii
N. bredini
N. festae
N. oerstedii
N. wennerae
H. californiensis
L. maculata
L. sulcata
S. empusa

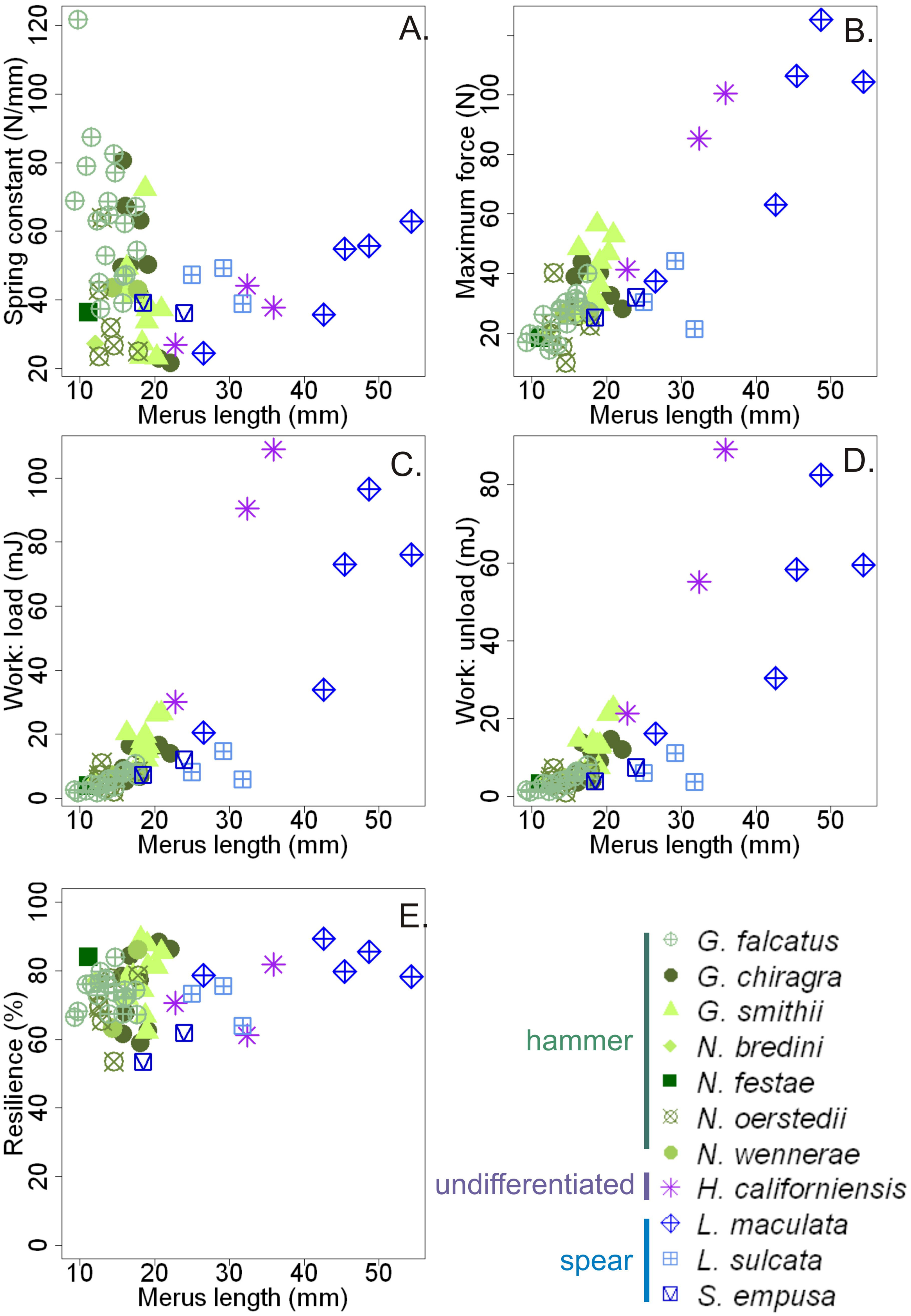
A.
Spring constant (N/mm)
20
40
60
80
100
120
Merus length (mm)
10
20
30
40
50
B.
Maximum force (N)
20
40
60
80
100
Merus length (mm)
10
20
30
40
50
C.
Work: load (mJ)
0
20
40
60
80
100
Merus length (mm)
10
20
30
40
50
D.
Work: unload (mJ)
0
20
40
60
80
Merus length (mm)
10
20
30
40
50
E.
Resilience (%)
0
20
40
60
80
100
Merus length (mm)
10
20
30
40
50
hammer
G. falcatus
G. chiragra
G. smithii
N. bredini
N. festae
N. oerstedii
N. wennerae
undifferentiated
H. californiensis
spear
L. maculata
L. sulcata
S. empusa

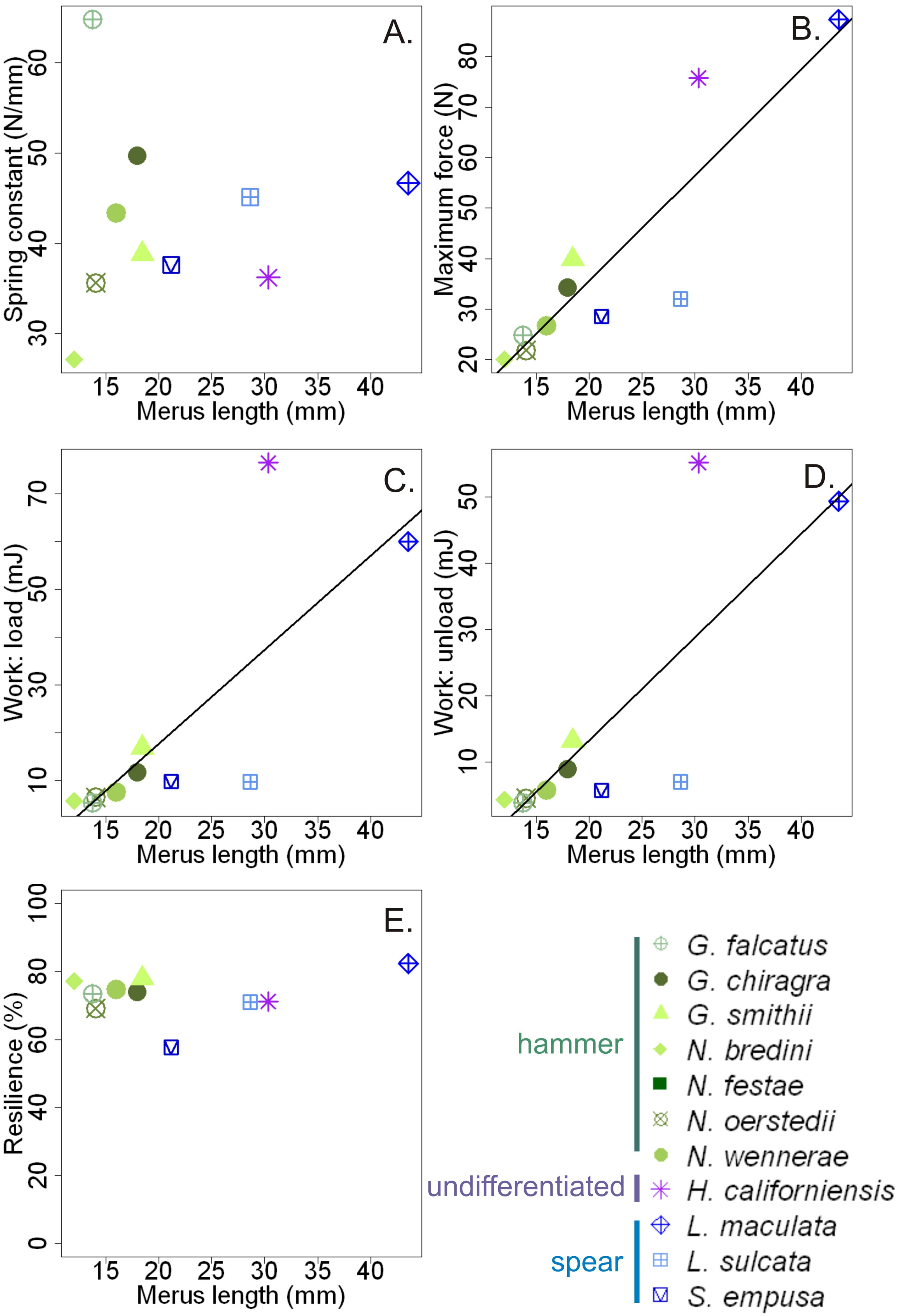

A.
Spring constant (N/mm)
30
40
50
60
B.
Maximum force (N)
20
30
40
50
60
70
80
C.
Work: load (mJ)
10
30
50
70
D.
Work: unload (mJ)
10
20
30
40
50
E.
Resilience (%)
0
20
40
60
80
100
15
20
25
30
35
40
Merus length (mm)
hammer
G. falcatus
G. chiragra
G. smithii
N. bredini
N. festae
N. oerstedii
N. wennerae
undifferentiated
H. californiensis
spear
L. maculata
L. sulcata
S. empusa

Table 1. Sample sizes, collection location, and body sizes of the species used in the study. The rate of appendage failure during materials tests is included; note that all *Pseudosquilla ciliata* failed during material testing. *N* is the number of individuals and *n* is the number of appendages tested that did not fail on the first pull. N_t and n_t are the total number of individuals and appendages tested respectively including failures. The appendage failure rate for *G. falcatus* is not reported, because failure data were not comparably recorded in the previous study (Zack et al., 2009). Row colors indicate appendage type (smashers: white; undifferentiated: dark-gray; spearers: light-gray).

Family	**Genus**	**Species**	***N(n)***	**$N_t(n_t)$**	**Mass (g)**	**Carapace length (mm)**	**Collection location**	**Appendage failure (%)**
Gonodactylidae	*Gonodactylaceus*	*falcatus*	18(18)	--	0.75-3.09	7.92-13.87	Oahu, Hawaii	na
Gonodactylidae	*Gonodactylus*	*chiragra*	13(10)	15(12)	3.00-11.00	12.43-19.39	Lizard Island, Australia	20
Gonodactylidae	*Gonodactylus*	*smithii*	12(11)	15(14)	3.60-6.60	13.84-17.31	Lizard Island, Australia	6.7
Gonodactylidae	*Neogonodactylus*	*bredini*	1(1)	1(1)	1.20	9.51	Isla Galeta, Panama	0
Gonodactylidae	*Neogonodactylus*	*festae*	1(1)	1(1)	1.00	8.58	Isla Naos, Panama	0
Gonodactylidae	*Neogonodactylus*	*oerstedii*	6(6)	7(7)	1.50-4.70	10.28-15.47	Isla Galeta, Panama	0
Gonodactylidae	*Neogonodactylus*	*wennerae*	3(2)	4(3)	2.30-3.70	11.37-13.56	Tampa Bay, Florida	25
Hemisquillidae	*Hemisquilla*	*californiensis*	11(3)	11(3)	29.91-102.21	23.71-35.55	Santa Catalina Island, California	72.7
Lysiosquillidae	*Lysiosquillina*	*maculata*	5(5)	5(5)	36.50-236	27.45-48.42	Lizard Island, Australia	0
Lysiosquillidae	*Lysiosquillina*	*sulcata*	3(3)	3(3)	39.90-50.80	26.94-29.51	Moorea, French Polynesia	0
Pseudosquillidae	*Pseudosquilla*	*ciliata*	4(0)	6(0)	3.81-4.88	14.23-15.23	Oahu, Hawaii	100
Squillidae	*Squilla*	*empusa*	2(2)	2(2)	9.72-20.30	18.84-23.79	Gulf Coast Research Laboratory, Mississippi	0

Table 2. Spring characteristics and size within each species. Results are presented as mean ± standard deviation (minimum – maximum). *one individual was missing body size data. N is the number of individuals tested per species. When two appendages were tested per individual, those two values are averaged to form one value for that individual. Row colors indicate appendage type (smashers: white; undifferentiated: dark-gray; spearers: light-gray).

Species	**N**	**Spring constant (N mm^{-1})**	**Max force (N)**	**Work: load (mJ)**	**Work: unload (mJ)**	**Resilience (%)**	**Body length (mm)**	**Merus length (mm)**
G. falcatus	18	64.78±20.49 (37.43-121.68)	24.87±7.04 (14.38-39.98)	5.32±2.76 (1.89-10.88)	3.88±1.98 (1.29-8.10)	73.51±4.80 (66.55-84.02)	45.28±6.66 (33.34-53.73)	13.76±2.46 (9.32-17.57)
G. chiragra	10*	48.90±18.49 (21.64-80.65)	34.17±6.27 (25.47-43.90)	11.70±4.28 (5.50-16.71)	8.88±4.09 (3.73-14.77)	73.90±10.83 (58.97-88.43)	62.29±8.71 (52.28-82.07)	17.96±2.24 (15.59-22.03)
G. smithii	11	38.80±13.84 (23.12-72.30)	39.84±10.69 (25.23-56.42)	16.81±6.26 (7.85-26.53)	13.16±5.39 (6.08-22.68)	77.92±8.47 (62.25-89.33)	62.11±4.70 (53.88-67.74)	18.45±1.47 (16.24-20.89)
N. bredini	1	27.14	20.08	5.64	4.35	77.26	38.18	12.05
N. festae	1	36.37	18.33	3.87	3.25	84.02	35.51	11.13
N. oerstedii	6	35.62±15.54 (23.56-63.91)	21.85±10.25 (10.01-40.22)	6.47±3.26 (2.07-11.13)	4.55±2.30 (1.11-7.26)	69.15±9.24 (53.55-78.72)	47.49±7.78 (39.14-61.73)	14.06±2.00 (12.50-17.76)
N. wennerae	2	43.33±0.42 (43.03-43.63)	26.77±0.34 (26.53-27.01)	7.58±0.31 (7.36-7.80)	5.75±1.37 (4.78-6.72)	74.77±16.14 (63.36-86.19)	49.93±4.64 (46.65-53.22)	16.01±2.38 (14.32-17.69)
H. californiensis	3	36.21±8.75 (26.80-44.10)	75.75±30.73 (41.38-100.58)	76.48±41.15 (30.18-108.86)	55.14±33.87 (21.30-89.05)	71.24±10.36 (61.20-81.89)	147.69±27.37 (118.97-173.47)	30.34±6.81 (22.74-35.90)
L. maculata	5	46.67±16.03 (24.38-62.81)	87.31±35.98 (37.38-125.24)	60.01±31.58 (20.57-96.48)	49.34±26.17 (16.18-82.51)	82.37±4.91 (78.35-89.44)	225.81±47.13 (147.03-266.71)	43.54±10.45 (26.56-54.37)
L. sulcata	3	45.12±5.50 (38.86-49.20)	31.99±11.53 (21.34-44.24)	9.673±4.56 (6.00-26.53)	7.01±3.75 (3.84-11.16)	70.97±6.13 (64.02-75.58)	158.13±8.56 (152.01-167.91)	28.63±3.45 (24.94-31.77)
S. empusa	2	37.63±2.04 (36.18-39.07)	28.57±4.82 (25.16-31.98)	9.74±3.29 (7.42-12.06)	5.72±2.49 (3.96-7.48)	57.73±5.98 (53.50-61.96)	97.41±15.24 (86.63-108.18)	21.16±3.87 (18.43-23.90)

Table 3. The ratios of spring parameters to merus length (ML) across species. Results are presented as mean ± standard deviation. *one individual was missing body size data. N is the number of individuals tested per species. When two appendages were tested per individual, those two values are averaged to form one value for that individual. Row colors indicate appendage type (smashers: white; undifferentiated: dark-gray; spearers: light-gray).

Species	**N**	**Spring constant/ML (N mm^{-1})**	**Max force/ML (N mm^{-1})**	**Work: load/ML (mJ mm^{-1})**	**Work: unload/ML (mJ mm^{-1})**	**Resilience/ML (% mm^{-1})**
G. falcatus	18	5.02±2.46	1.80±0.35	0.37±0.14	0.27±0.10	5.51±1.05
G. chiragra	10*	2.90±1.34	1.94±0.46	0.64±0.23	0.49±0.22	4.15±0.64
G. smithii	11	2.13±0.81	2.15±0.54	0.90±0.30	0.70±0.25	4.24±0.50
N. bredini	1	2.25	1.67	0.47	0.36	6.41
N. festae	1	3.27	1.65	0.35	0.29	7.55
N. oerstedii	6	2.63±1.33	1.60±0.85	0.47±0.25	0.33±0.17	4.97±0.77
N. wennerae	2	2.74±0.43	1.69±0.23	0.48±0.05	0.36±0.03	4.65±0.32
H. californiensis	3	1.20±0.16	2.42±0.53	2.38±0.92	1.71±0.77	2.43±0.62
L. maculata	5	1.05±0.16	1.94±0.51	1.31±0.52	1.08±0.44	2.00±0.58
L. sulcata	3	1.60±0.34	1.14±0.43	0.34±0.16	0.25±0.13	2.52±0.47
S. empusa	2	1.82±0.43	1.35±0.02	0.45±0.07	0.26±0.07	2.75±0.22

Table 4. The relationships between merus length as the independent variable and spring characteristics as the dependent variables across species, calculated using Phylogenetic Generalized Least Squares with mean species values. The statistical results apply to the coefficient. None of the intercepts are significantly different from zero, except for resilience (t=13.043, p=0.0000). Statistically significant values are indicated in bold. The results of using the combined males and females dataset are presented here; males only and females only datasets yield qualitatively similar results with the exception of resilience in females (**λ** =1 ; intercept: 60.7; coeff.: 0.71; std.err.: 0.15; p=0.0045). **λ** represents phylogenetic correlation ranging from 0 (no phylogenetic signal) to 1 (Brownian motion) (Freckleton et al., 2002; Pagel, 1999). **λ** is 0 for the data shown here.

	Intercept	**Coefficient**	**Standard error**	**t-value**	**P-value**
Spring constant (N mm^{-1})	37.93	0.17	0.39	0.4403	0.6713
Maximum force (N)	**-6.17**	**2.09**	**0.36**	**5.8498**	**0.0004**
Work: load (mJ)	**-21.69**	**1.97**	**0.53**	**3.6819**	**0.0062**
Work: unload (mJ)	**-17.87**	**1.56**	**0.39**	**4.0265**	**0.0038**
Resilience (%)	70.68	0.11	0.24	0.4758	0.6470

Table 5. The scaling of spring characteristics relative to merus length within each species using a least-squares linear regression. Statistically significant values are indicated in bold. *L. maculata* (gray) is a spearer; the remaining species are smashers.

	Species	**Intercept**	**Slope**	**F-statistic**	**df**	**P-value**	**R^2**
Spring constant ($N\ mm^{-1}$)	***falcatus***	**121.35**	**-4.11**	**5.14**	**1,16**	**0.0376**	**0.2431**
	chiragra	**176.66**	**-7.07**	**13.74**	**1,7**	**0.0076**	**0.6625**
	smithii	88.33	-2.68	0.79	1,9	0.3960	0.0811
	oerstedii	84.73	-3.49	1.01	1,4	0.3713	0.2019
	maculata	**-15.68**	**1.43**	**20.24**	**1,3**	**0.0205**	**0.8709**
Maximum force (N)	***falcatus***	**-4.37**	**2.12**	**19.59**	**1,16**	**0.0004**	**0.5504**
	chiragra	41.92	-0.42	0.15	1,7	0.7134	0.0205
	smithii	-24.45	3.48	2.67	1,9	0.1364	0.2291
	oerstedii	38.90	-1.21	0.24	1,4	0.6517	0.0560
	maculata	-41.03	2.95	8.23	1,3	0.0642	0.7327
Work: load (mJ)	***falcatus***	**-7.90**	**0.96**	**43.27**	**1,16**	**0.0000**	**0.7301**
	chiragra	-9.71	1.19	3.69	1,7	0.0964	0.3449
	smithii	**-35.54**	**2.84**	**7.16**	**1,9**	**0.0254**	**0.4429**
	oerstedii	6.92	-0.03	0.00	1,4	0.9708	0.0004
	maculata	-47.59	2.47	6.05	1,3	0.0908	0.6686
Work: unload (mJ)	***falcatus***	**-5.58**	**0.69**	**43.45**	**1,16**	**0.0000**	**0.7309**
	chiragra	-12.17	1.17	4.06	1,7	0.0836	0.3673
	smithii	**-34.76**	**2.60**	**9.00**	**1,9**	**0.0150**	**0.4999**
	oerstedii	2.56	0.14	0.06	1,4	0.8162	0.0152
	maculata	-38.09	2.01	5.39	1,3	0.1028	0.6426
Resilience (%)	*falcatus*	73.27	0.02	0.00	1,16	0.9713	0.0001
	chiragra	34.19	2.22	1.61	1,7	0.2446	0.1873
	smithii	52.04	1.40	0.57	1,9	0.4712	0.0591
	oerstedii	46.73	1.60	0.54	1,4	0.5028	0.1191
	maculata	79.92	0.06	0.04	1,3	0.8479	0.0143

Table 6. The effects of cutting the saddle on spring characteristics across species. Paired t-tests were performed, except when data were not normally distributed. *In this latter case, a paired Wilcoxon signed rank test was performed (indicated by "V=") in the t-value column. Statistically significant values are indicated in bold. *L. maculata* is a spearer (gray); the remaining species are smashers.

	Species	**t-value***	**df**	**P-value**	**Mean of differences**
Spring constant (N mm^{-1})	***falcatus***	**4.2373**	**13**	**0.0010**	**4.45**
	chiragra	0.6211	9	0.5499	1.07
	smithii	-1.2008	10	0.2575	-1.18
	oerstedii	1.3386	5	0.2383	8.01
	maculata	-1.7609	3	0.1765	-14.25
Maximum force (N)	***falcatus***	**8.0989**	**13**	**0.0000**	**3.60**
	chiragra	**6.1219**	**9**	**0.0002**	**5.31**
	smithii	**V = 61**		**0.0098**	**4.23**
	oerstedii	1.7444	5	0.1415	6.46
	maculata	V = 1		0.2500	-32.05
Work: load (mJ)	***falcatus***	**5.6182**	**13**	**0.0001**	**0.99**
	chiragra	**4.6379**	**9**	**0.0012**	**2.38**
	smithii	**3.413**	**10**	**0.0066**	**2.37**
	oerstedii	1.9583	5	0.1075	1.96
	maculata	-2.1381	3	0.1221	-21.75
Work: unload (mJ)	***falcatus***	**4.5751**	**13**	**0.0005**	**0.59**
	chiragra	**4.0228**	**9**	**0.0030**	**1.58**
	smithii	**2.9778**	**10**	**0.0139**	**1.84**
	oerstedii	1.8299	5	0.1268	1.24
	maculata	-2.0155	3	0.1372	-18.06
Resilience (%)	***falcatus***	**-3.7337**	**13**	**0.0025**	**-2.57**
	chiragra	**-3.2098**	**9**	**0.0107**	**-1.98**
	smithii	-0.3516	10	0.7324	-0.53
	oerstedii	-1.8154	5	0.1292	-2.79
	maculata	0.2508	3	0.8182	0.37

Table 7. Percent change in spring parameter after the saddle was severed; negative values indicate a decrease after the saddle was cut. Individual values were calculated and then averaged to generate species means. Row colors indicate appendage type (smashers: white; undifferentiated: dark-gray; spearers: light-gray).

Species	**n**	**Spring constant**	**Maximum force**	**Work: load**	**Work: unload**	**Resilience**
falcatus	14	-6.5	-13.4	-15.8	-12.7	3.6
chiragra	9	-0.4	-16.4	-21.3	-19.4	2.5
smithii	11	4.0	-10.0	-13.3	-12.6	0.8
bredini	1	-3.2	-23.1	-27.5	-27.0	0.5
festae	1	6.0	-15.8	-21.0	-22.4	-1.7
oerstedii	6	-13.5	-21.8	-24.3	-20.1	4.6
wennerae	2	-15.5	-7.7	-0.7	8.4	8.9
californiensis	1	-17.1	-21.5	-21.0	-18.9	2.6
maculata	4	-27.7	-35.0	-34.7	-34.3	0.5
sulcata	1	-38.6	-20.3	-1.3	-1.5	-0.4
empusa	2	-33.5	-30.1	-28.1	-19.5	11.7

Table 8. The scaling of spring characteristics relative to merus length in two different datasets - one including only species with spears and the other consisting of species with hammers. The analyses were calculated using Phylogenetic Generalized Least Squares with mean species values. The statistical results apply to the coefficient. None of the intercepts are significantly different from zero, except for the spring constant in spearers (t=6.23, p=0.0248) and resilience in species with hammers (t=8.08, p=0.0013). **λ** represents phylogenetic correlation ranging from 0 (no phylogenetic signal) to 1 (Brownian motion) (Freckleton et al., 2002; Pagel, 1999). Assumptions were violated for the resilience calculation in spearers, so those values are not included. Row colors indicate appendage type (smashers: white; spearers: light-gray). Statistically significant values are indicated in bold.

	Intercept	**Coefficient**	**Standard error**	**t-value**	**P-value**	**λ**
Spring constant (N mm^{-1})	33.23	0.51	1.98	0.26	0.8083	1
	27.47	0.40	0.09	4.26	0.0509	1
Maximum force (N)	**-14.58**	**2.77**	**0.46**	**6.01**	**0.0039**	**0**
	-18.58	**2.65**	**0.37**	**7.07**	**0.0194**	**1**
Work: load (mJ)	**-13.78**	**1.48**	**0.40**	**3.73**	**0.0203**	**0**
	-16.28	2.27	0.58	3.89	0.0602	1
Work: unload (mJ)	**-11.16**	**1.17**	**0.33**	**3.52**	**0.0244**	**0**
	-21.36	**1.97**	**0.42**	**4.73**	**0.0419**	**1**
Resilience (%)	72.94	0.11	0.59	0.19	0.8574	0
	na	na	na	na	na	na